https://doi.org/10.1016/j.apenergy.2020.116038

Energy planning of renewable applications in high-rise residential buildings integrating battery and hydrogen vehicle storage

Jia Liu [a*], Sunliang Cao [a, b], Xi Chen [c], Hongxing Yang [a*], Jinqing Peng [d]

[a] Renewable Energy Research Group (RERG), Department of Building Services Engineering, The Hong Kong Polytechnic University, Kowloon, Hong Kong, China

[b] Research Institute for Sustainable Urban Development (RISUD), The Hong Kong Polytechnic University, Kowloon, Hong Kong, China

[c] School of Science and Technology, The Open University of Hong Kong, Hong Kong, China

[d] College of Civil Engineering, Hunan University, Changsha, Hunan, China

Abstract

This study presents a robust energy planning approach for hybrid photovoltaic and wind energy systems with battery and hydrogen vehicle storage technologies in a typical high-rise residential building considering different vehicle-to-building schedules. Multiple design criteria including the supply performance, grid integration and lifetime net present value are adopted to size the hybrid system and select the optimal energy management strategy. Four decision-making strategies are further applied to search the final optimum solution for major stakeholders with different preferences. The study result indicates that the energy management strategy with battery storage prior to hydrogen storage is suitable for hybrid systems with large photovoltaic, wind and battery installation capacities to achieve the optimum supply-grid integration-economy performance. The energy management strategy with hydrogen storage prior to battery storage has a wider applicability, and this strategy should be selected when focusing on the supply-grid integration or supply-economy performance. The annual average self-consumption ratio, load cover ratio and hydrogen system efficiency are about 84.79%, 76.11% and 77.06% respectively in the end-user priority case. The annual absolute net grid exchange is about 4.55 MWh in the transmission system operator priority case. The lifetime net present value of the investor priority case is about 3.64 million US$, 29.88% less than the equivalent priority case. Final optimum solutions show positive environmental impacts with negative annual carbon emissions. Such a techno-economic-environmental feasibility analysis of the hybrid system provides major

* Corresponding author 1: jiajia.liu@connect.polyu.hk
* Corresponding author 2: hong-xing.yang@polyu.edu.hk

stakeholders with valuable energy planning references to promote renewable applications in urban areas.

Keywords

Solar photovoltaic; Wind turbine; Battery storage; Hydrogen vehicle; High-rise building; Energy planning

1. Introduction

1.1. Background

Renewable energy is playing an expanding role in the power sector [1] and providing about 27.3% of global electricity generation accumulating to 2588 GW at the end of 2019 [2]. It has been adopted as a global-scale decarbonisation pathway towards the low-carbon power supply and sustainable environment especially in crucial sectors with high carbon emissions and energy consumption such as the building and transport. Most carbon emissions in Hong Kong are attributed to electricity generation (70%) and transport (16%) sectors, while 90% of electricity is consumed by buildings [3]. More than half of the total energy consumption of Hong Kong is attributed to the residential (21%) and transport (31%) sectors in 2017, and the energy and electricity consumption of the residential sector shows a continuous rise from 2007 to 2017 by 9.6% and 15.7% respectively [4]. The local government has therefore launched ambitious plans to achieve an absolute carbon reduction of 26% - 36% by 2030 benchmarked with 2005. It is significant to accelerate renewable energy development as it accounts for only 0.2% of total local electricity consumption in 2017 [4], while 3% - 4% of the renewable energy supply has been planned [3]. The hybrid renewable energy and storage systems with complementary photovoltaic (PV) and wind power combined with lithium-ion battery storage and hydrogen vehicles are thus developed for power supply to high-rise residential buildings.

Batteries have been widely adopted for renewable energy storage in buildings given its fast response, high efficiency and low environmental impact [5], while hydrogen is attracting increasing attention in many economic sectors given its low-carbon characteristics. The lower heating value of hydrogen is about 120 MJ/kg (3 times of gasoline), which makes it an attractive transport fuel. But hydrogen needs to be compressed or liquefied as the energy intensity of hydrogen is relatively low at 0.01 MJ/L (1/3 of natural gas) [6]. This study adopts a vehicle

integrated hydrogen storage system consisting of the alkaline electrolyzer, compressor, hydrogen storage tank and proton exchange membrane fuel cell (PEMFC) for the hybrid renewable energy system. The alkaline electrolyzer has been used since the 1920s as a commercial and mature technology with a relatively low initial cost (500 - 1400 US$/kW) compared with other electrolyzers such as the proton exchange membrane electrolyzer (1100 - 1800 US$/kW) and solid oxide electrolyzer (2800 - 5600 US$/kW) [7]. The electrical efficiency of alkaline electrolyzer at the lower heating value is about 63% - 70% depending on the technology performance and supply power, and it is projected to be increased to 70% - 80% in the long-term development. The hydrogen fuel cell costs 1600 US$/kW for a 1 MW PEMFC unit with an electrical efficiency of 50% - 60% and it is predicted to be reduced to about 425 US$/kW by 2030 [8]. It is therefore technically and economically promising to develop hybrid renewable energy and storage systems integrating the building and transport sectors.

1.2. Global development status and prospects of hydrogen vehicles

Recently, hydrogen vehicles (HVs) have experienced an unprecedented development as a promising alternative for clean energy solution. Over 12900 fuel cell electric cars are registered worldwide by the end of 2018 with an 80% increment in the year, although still small compared with the accumulated 5.1 million battery vehicles. Nearly half of HVs are sold in the U.S., followed by 23% in Japan and 14% in China, while most HVs are manufactured by Toyota, Honda and Hyundai. There are 376 publicly available hydrogen refueling stations with 100 in Japan, followed by 60 in Germany and 44 in the U.S [9], but the number is still small compared with the 5.2 million charging points (90% private chargers) for battery vehicles by the end of 2018 [10]. HVs can be refueled in 3 - 5 minutes, much shorter than that of battery vehicles (can be 3 - 6 hours) and fuel cells could have a lower material footprint than lithium batteries. The cruise range of HVs can be over 400 km, longer than that of battery vehicles with a global average around 250 km [6]. A promising global development of HVs is anticipated in the near future to achieve a low-carbon transport sector. The Korean government aims to achieve 6.2 million HVs and 1200 refueling stations by 2040 and make hydrogen economy a driving force of innovation growth [11]. About 20000 - 50000 HVs and 400 - 1000 refueling stations are projected by 2028 in France and 1000 refueling stations will be constructed in Germany [9]. Up to 1 million fuel cell electric vehicles and 1000 hydrogen refueling stations will be developed by 2030 in China to launch the hydrogen

transport in ten cities following exiting battery vehicles [12]. A similar plan is outlined by the California Fuel Cell Partnership to encourage the development of low-carbon hydrogen in California [13]. Japan also planned to have 0.2 million HVs and 320 refueling stations by 2025 with accumulated HVs of 0.8 million by 2030 [14]. Hydrogen Council anticipates more than 400 million hydrogen cars, 15 - 20 million hydrogen trucks and 5 million hydrogen buses all over the world by 2050 [15].

1.3. Review of integrating battery and hydrogen storage with renewable energy systems for building power supply

Feasibility and optimization studies on battery and hydrogen storage based renewable energy systems for building power supply have aroused increasing attention in recent years with an accelerating development of battery and hydrogen technologies in energy storage and transportation.

The technical and economic feasibility of employing battery and hydrogen storage based renewable energy systems for building power supply has been investigated based on case studies and parametric analyses. A standalone plug-in hybrid electric vehicle charging station powered by PV and wind energy with fuel cell storage is tested showing that the lifetime and cost of the fuel cell system are more favorable than that of the battery system [16]. A demonstration project with the solar PV and fuel cell electric vehicle in a residential building was set up in the Netherlands to study the net zero-energy and vehicle-to-grid operations. It is found that the annual grid imported electricity can be reduced by 71% with the integration of the fuel cell vehicle [17]. The technical and economic performance of a PV-wind system with vehicle integrated hydrogen storage is analyzed for a zero-emission single family house in Finland considering the system net present value and operational carbon emissions [18]. The vehicle integrated hydrogen storage and battery storage are designed for solar and wind systems in a practical office center of the Netherlands. This study validated the feasibility of using electric vehicles as the power backup as well as the flexibility and cost-effectiveness of fuel cell vehicles over battery vehicles [19]. The power generation planning of isolated microgrids with diesel and renewable energy sources is presented considering the integration of electric vehicles and cooking systems. The economic and environmental benefits of the renewable energy system for a remote community in Ecuador are demonstrated based on the HOMER analysis [20]. The impact of vehicle-to-building interactions

and vehicle charging strategies on the performance of zero-emission office buildings is analyzed. The author reports that the matching capability and building-vehicle interactions can be significantly improved by expanding the vehicle charging boundary to remote parking sites [21].

A large amount of research has also been conducted on the sizing and design optimization of battery and hydrogen storage based renewable energy systems for building power supply in both standalone and grid-connected conditions. For example, the PV system with hydrogen and retired vehicle battery storage is developed for a typical household in China by optimizing the energy supply reliability, energy waste and system cost. The superiority of Non-dominated Sorting Genetic Algorithm-II (NSGA-II) is explicated in this study compared with the multi-objective evolutionary algorithm based on decomposition [22]. The widely used metaheuristics are further compared in optimizing and sizing a micro-grid hybrid PV-wind-hydro system with supercapacitor storage and hydrogen refueling station for fuel cell vehicles in a New Zealand community. The authors conclude that the moth-flame optimization algorithm gets the best solution in cost effectiveness with a 0.09 US$/kWh levelized cost of electricity [23]. Three operation strategies of the PV-battery-hydrogen system are developed under the pessimistic and optimistic cost scenarios for a multi-apartment building in Sweden, showing that hydrogen storage performs better than battery storage in the net present value under the optimistic cost scenario [24]. The optimal design and operation of the hybrid solar-hydro system with stationary hydrogen storage is also analyzed based on General Algebraic Modeling System (GAMS) for a net-zero energy building to minimize the investment of the solar system. A carbon dioxide reduction of 39546 kg and cost decline of 50.3% can be achieved by the optimum design [25]. An innovative optimization model is proposed for investment planning of a renewables microgrid with electric vehicles. Case studies of microgrid systems with a 5-year planning horizon show that the vehicle-to-grid technology contributes to the microgrid economy in the long-term operation [26]. A microgrid planning algorithm of renewable energy systems integrating electric vehicles is proposed to maximize renewable generations. It is found that the developed algorithm can reduce the investment cost and carbon emission for residential and campus microgrids cases in Korea [27]. Both single-objective and multi-objective optimizations are conducted to improve the technical, economic and environmental performance of a low-energy building integrated with the PV and battery storage system considering the battery cycling aging, grid relief and time-of-use pricing [28].

Table 1 A summary of recent studies on battery and hydrogen storage based renewable energy systems

Hybrid system	Software	Application site	Important finding	Reference
Feasibility analysis				
PV-wind-stationary hydrogen	--	A standalone hybrid vehicle charging station	Lifetime and cost of fuel cell system are more favorable than battery system	Fathabadi. 2020 [16]
PV-mobile hydrogen vehicle	MATLAB	Vehicle-to-grid, the Netherlands	Annual grid imported electricity can be reduced by 71% using fuel cell vehicle	Robledo et al. 2018 [17]
PV-wind-mobile hydrogen vehicle	TRNSYS	An on-grid single family house, Finland	Techno-economic feasibility of using HV in a zero-energy building is explained	Cao et al. 2018 [18]
PV-wind-mobile hydrogen vehicle	MATLAB	An on-grid office center, the Netherlands	Fuel cell vehicles are more economic and flexible than battery vehicles	Farahani et al. 2020 [19]
PV-wind-mobile battery vehicle	HOMER	An island community microgrid, Ecuador	Economic and environmental benefits can be obtained integrating renewables and electric vehicles in island microgrids	Clairand et al. 2019 [20]
PV-wind-mobile battery vehicle	TRNSYS	An on-grid office building, Hong Kong	Matching capability and building-vehicle interactions are improved by expanding the mobile boundary	Cao 2019 [21]
Design sizing and optimization				
PV-stationary hydrogen-retired vehicle battery	HOMER	A standalone neighborhood, China	NSGA-II performs better than multi-objective evolutionary algorithm based on decomposition	Huang et al. 2019 [22]
PV-wind-hydro-supercapacitor-stationary hydrogen	MATLAB	A rural community, New Zealand	Moth-flame optimization algorithm gets the best solution in cost effectiveness	Mohseni et al. 2020 [23]
PV-stationary battery-stationary hydrogen	MATLAB	An on-grid rental building, Sweden	Hydrogen storage is more economic under optimistic cost scenario than battery storage	Zhang et al. 2017 [24]
PV-hydro-stationary hydrogen	GAMS	An off-grid net-zero energy building	Carbon dioxide and cost reduction can be achieved by the optimum design	Mehrjerdi et al. 2019 [25]

Hybrid system	Software	Application site	Important finding	Reference
PV-wind-mobile battery vehicle	IBM CPLEX and Matpower	Vehicle-to-grid parking facilities	Vehicle-to-grid technology contributes to the microgrid economy in the long-term operations	Mortaz et al. 2019 [26]
PV-wind-mobile battery vehicle	HOMER	Residential and campus microgrids, Korea	Investment cost and CO_2 emission can be reduced by the proposed algorithm	Yoon et al. 2017 [27]
PV-stationary battery	TRNSYS, jEplus+EA	An on-grid low-energy building, China	Technical, economic and environmental performance can be improved by the optimizations	Liu et al. 2020 [28]

Table 1 summaries recent research on the feasibility and optimization study of battery and hydrogen storage (both stationary and mobile types) based renewable energy systems for building applications. It can be identified that few techno-economic feasibility studies focus on high-rise building applications within the urban context considering different transporting schedules of hydrogen vehicle groups. And most existing design optimization studies are limited to stationary hydrogen storage. Moreover, optimum sizing schemes and energy management strategies of hybrid renewable energy systems with battery and hydrogen vehicle storage are seldom presented for major stakeholders considering their different concerns.

1.4. Scope and contribution

Given the identified research gap, this study presents a robust energy planning approach for the hybrid PV-wind-battery-hydrogen system for power supply to high-rise residential buildings integrated with hydrogen vehicles in different cruise schedules. The preferences of key stakeholders are addressed for decision making for different energy management strategies based on the joint TRNSYS and jEplus+EA platform. Major contributions of the present study are shown as below:

(1) Two energy management strategies of the hybrid PV-wind-battery-hydrogen system with different operation priorities of the battery storage and hydrogen storage are developed and compared for power supply to a typical high-rise residential building integrated with two groups of hydrogen vehicles following different cruise schedules. The energy management strategies and

system configurations are optimized considering the system supply performance, grid integration and lifetime net present value based on multi-objective design optimizations.

(2) Four decision-making strategies based on the minimum distance to the utopia point and analytical hierarchy process methods are adopted to determine the final optimum solutions for major stakeholders (i.e. the end-user, transmission system operator and investor) of hybrid renewable energy and storage systems for high-rise residential building applications within urban contexts.

(3) The techno-economic-environmental feasibility of four optimum solutions of the hybrid PV-wind-battery-hydrogen system with different concerns under the optimal energy management strategy is analyzed to provide valuable references for key stakeholders to further develop hybrid renewable energy and storage systems in urban areas.

2. Methodology

The hybrid renewable energy and storage system is first established in TRNSYS 18 [29] to model power supply to a typical high-rise residential building in Hong Kong with two groups of hydrogen vehicles (HVs) following different cruise schedules as per Fig. 1. The hybrid renewable energy supply adopts a combination of solar PV and wind power systems given their good complementary characteristics [30]. Solar PV panels are assumed to be installed on the rooftop and three vertical facades. The hybrid storage technologies consisting of lithium-ion battery energy storage (BES) and vehicles integrated hydrogen energy storage (HES) are utilized to match with the hybrid renewable energy supply. The battery technology is widely adopted for renewable energy storage in buildings given its fast response, high efficiency and low environmental impact [5], while the hydrogen vehicle technology meets well with the low-carbon development plan in the building and transportation sectors of Hong Kong [3]. The batteries equipped in the building can be charged by available renewable energy and discharged to meet the electrical load. The hydrogen system includes the electrolyzers, compressors, stationary hydrogen (H_2) storage tank fixed in the building and two groups of mobile hydrogen vehicles (HVs) with a H_2 storage tank and proton exchange membrane fuel cell (PEMFC) in each HV. The two groups of mobile HVs with different cruise schedules can be discharged to meet the electrical load when parking at home. And the heat release of the hydrogen system is recovered from the electrolyzers, compressors and PEMFCs for the air-conditioning reheat and domestic hot water demand to enhance the overall

efficiency of the HES system. The utility grid is connected to the hybrid PV-wind-battery-hydrogen system to take in surplus renewable generation, cover the unmet electrical load and supply power to the hydrogen system for necessary daily cruise consumption.

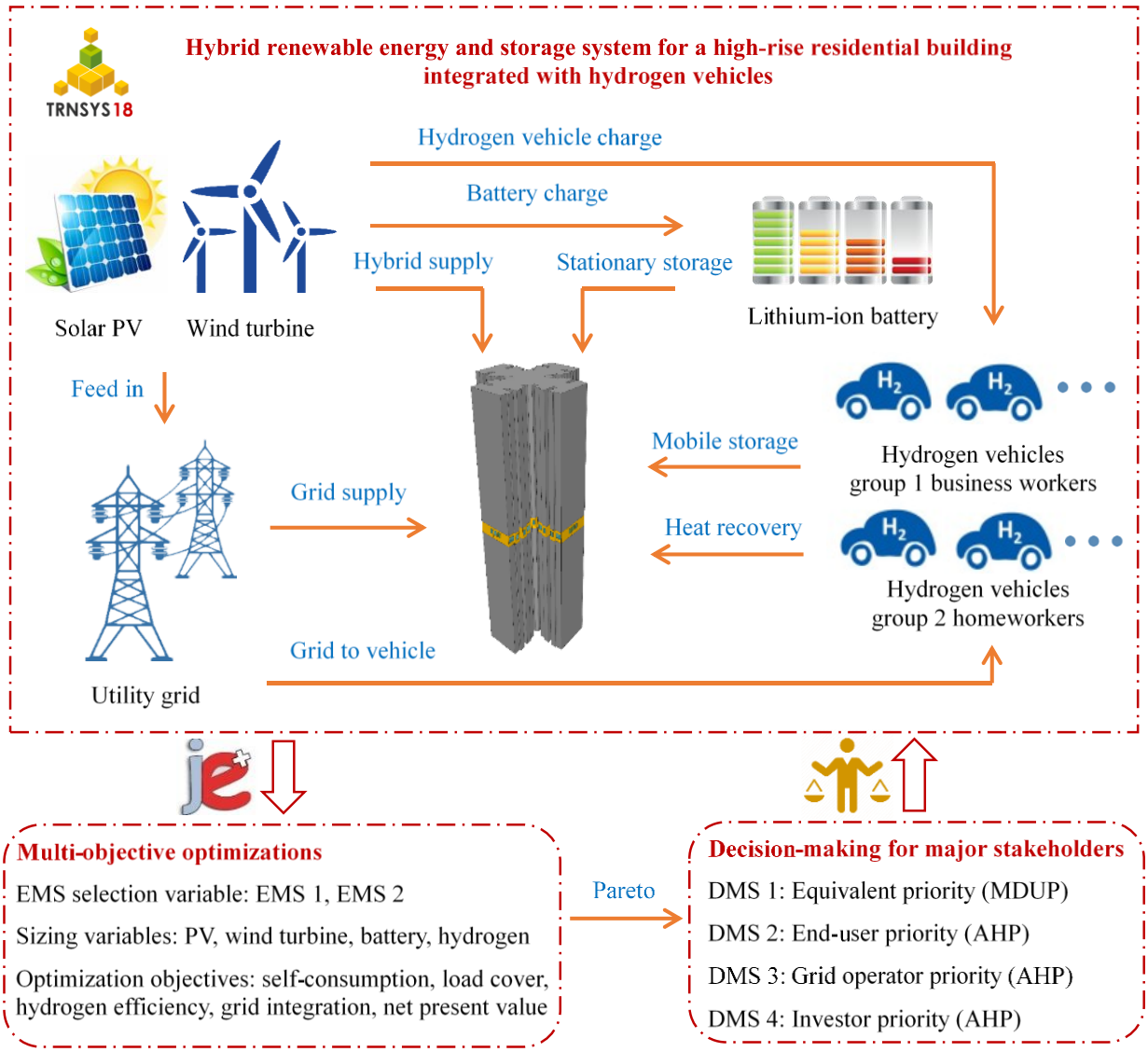

Fig. 1 Framework of the hybrid PV-wind-battery-hydrogen system for the high-rise building

Two energy management strategies (EMSs) are developed with different operation priorities of the storage technologies, where BES is prioritized over HES in EMS 1 and HES is prioritized in EMS 2. Multi-objective optimizations are conducted with the joint simulation and optimization platform of TRNSYS and jEplus+EA to select the optimum EMS and configuration of the hybrid PV-wind-battery-hydrogen system regarding the façade PV area, wind turbine number, battery capacity and stationary H_2 storage tank volume. Techno-economic indicators are developed for the

multi-objective optimization covering the self-consumption of renewable energy, on-site cover of the electrical load, overall efficiency of the hydrogen system, absolute value of net grid exchange and lifetime net present value. Four decision-making strategies (DMSs) are adopted to find the final optimum solution focusing on different concerns of major stakeholders from Pareto optimal solutions. Specifically, DMS 1 assigns equivalent priority to all design criteria based on the minimum distance to the utopia point (MDUP) method. DMSs 2 - 4 focus on the preference of the end-user, transmission system operator and investor respectively based on the analytical hierarchy process (AHP) method.

2.1. Modelling of hybrid renewable energy and storage system for hydrogen vehicle integrated building

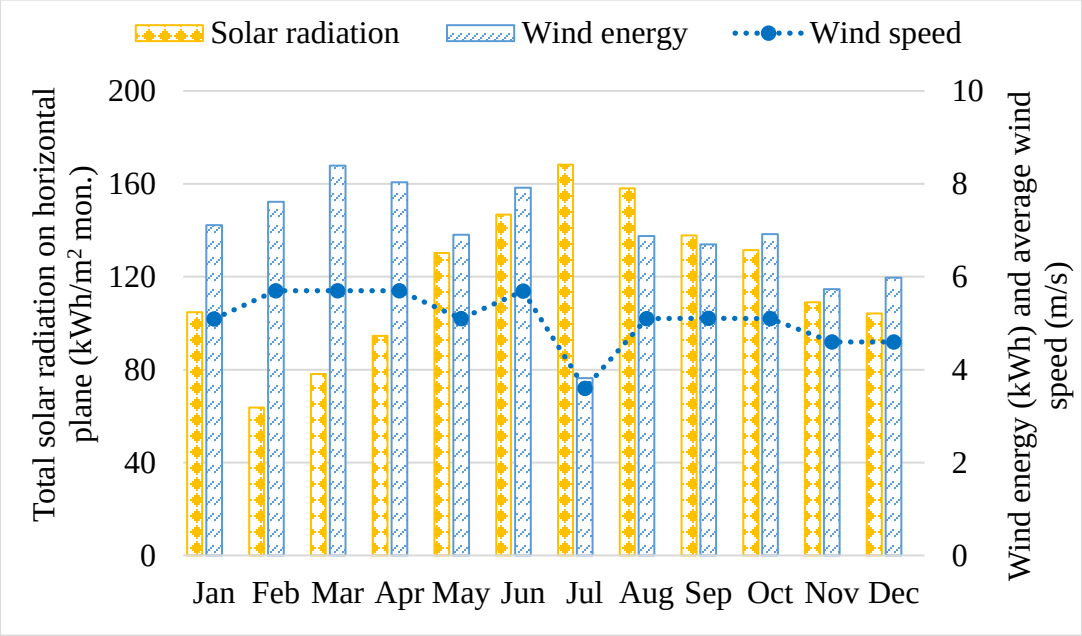

Fig. 2 Monthly solar radiation, wind energy (100 kW) and average weed speed in Hong Kong

The high-rise building is located in Hong Kong with favorable solar and wind resources as shown in Fig. 2 according to the weather file of TRNSYS 18 based on the Meteonorm data of Hong Kong [31]. The monthly solar radiation on the horizontal plane varies between 63.73 - 168.22 kWh/m^2 reaching the minimum and maximum in February and July respectively. While a 100 kW offshore wind turbine can generate more energy in winter and less in summer with the minimum and maximum monthly average wind speed of 3.60 m/s (July) and 5.70 m/s (March)

respectively. It is therefore promising to combine solar and wind energy for a stable renewable power supply to buildings given their complementary characteristics in Hong Kong.

A typical high-rise residential building with 30 floors (8 two-occupant flats and 8 four-occupant flats in each floor) is constructed based on a standard design layout for public residential buildings in Hong Kong [32]. The building envelope, air-conditioning load, internal gain and domestic hot water demand are specified as per local building codes [33]. The detailed load profile is obtained using internal models in TRNSYS 18 including Type 56, Type 648, Type 667, Type 752, Type 655 and other auxiliary components. The annual load of the high-rise building is simulated at a timestep of 0.125 h with detailed monthly results shown in Fig. 3. The internal gain load of 41.19 kWh/m^2 includes the electrical demand of indoor lighting, equipment and ventilation fans. The annual cooling load from April to October is about 41.99 kWh/m^2 and annual domestic hot water demand is 47.06 kWh/m^2, which agrees well with a survey on the annual average energy use intensity of high-rise residential buildings in Hong Kong [34].

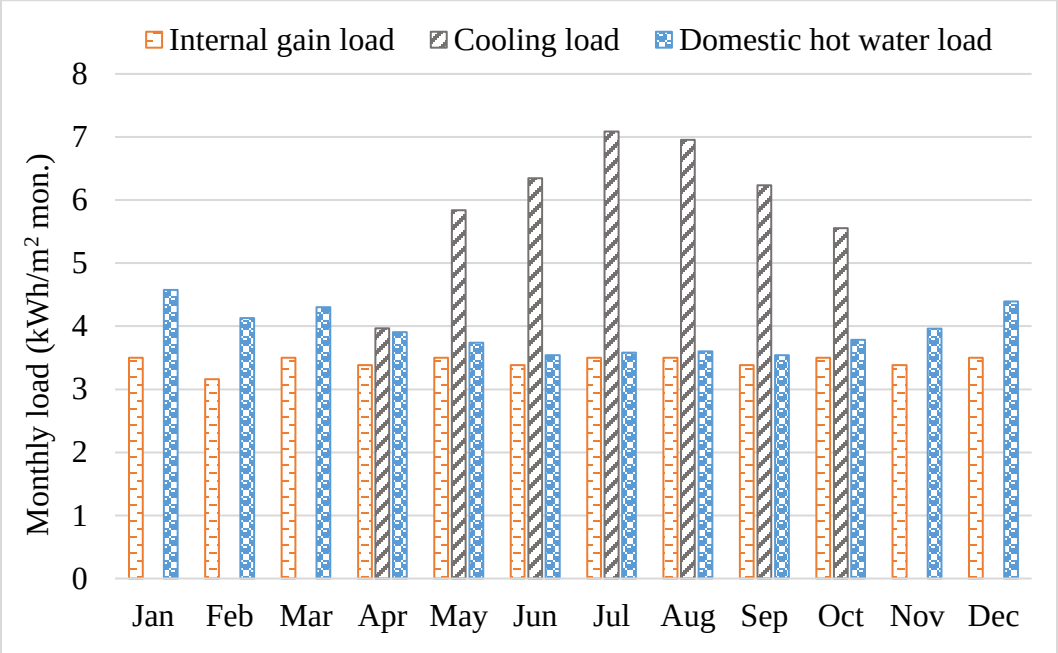

Fig. 3 Monthly electrical load of the high-rise residential building

Fig. 4 is a schematic of the hybrid PV-wind-battery-hydrogen system for the HVs integrated building. Detailed information of the hybrid supply, battery energy storage (BES), hydrogen energy storage (HES) and energy management strategy (EMS) is explained as below.

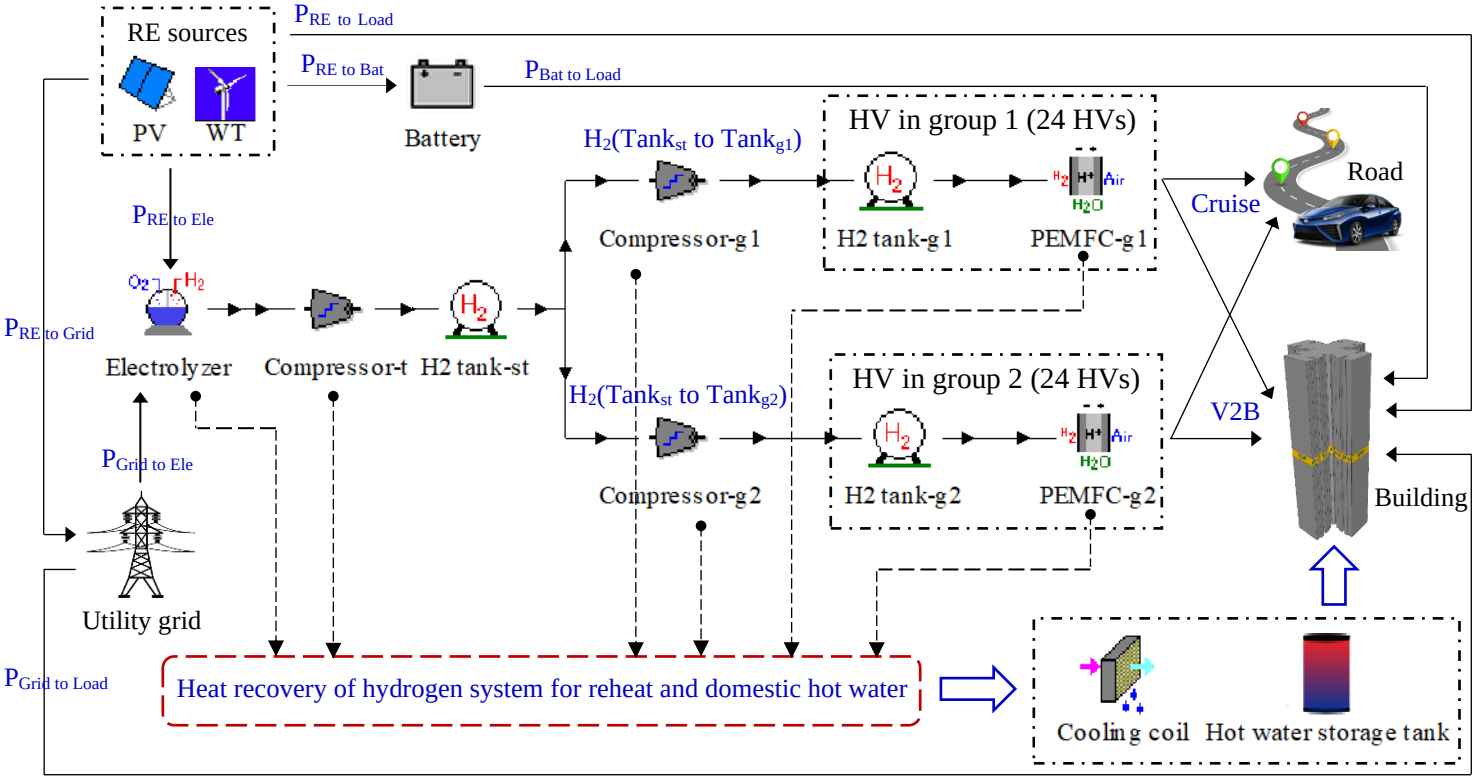

Fig. 4 Schematic of the hybrid PV-wind-battery-hydrogen system for the high-rise building

Hybrid supply: Rooftop PV panels are modelled by TRNSYS Type 103 with a tilted angle of 22º close to the local latitude and a capacity of about 70.76 kW. Façade PV panels are simulated by TRNSYS Type 567 and assumed to be installed on three building façades excluding North. The installation capacity is a design variable in sizing the hybrid system considering techno-economic indicators from the perspective of different stakeholders. An adjacent shading factor of 76.64% is introduced to model the façade PV power generation within the urban context [35]. Wind turbines are also modelled by TRNSYS Type 90 based on the tested power-speed characteristic curve from manufacturers as the supplementary power supply [36]. The installation capacity of wind power is also subject to further optimizations considering different stakeholders' concerns assuming a power transmission loss rate of 13.541% for the residential building in populated regions [37].

***Battery energy storage* (*BES*)**: The batteries are assumed to be installed in the building and subject to design optimization considering preferences of different stakeholders. It can be charged

by surplus renewable energy or discharged to meet the electrical load by controlling the fractional battery state of charge (FSOC) with an operational limit between $FSOC_{Bat\_min}$ - $FSOC_{Bat\_max}$ (0.15 - 0.98). The maximum charging and discharging rate of the battery is also considered according to the battery characteristic (i.e. 1C for the lithium-ion battery) [38].

***Hydrogen energy storage* (*HES*)**: 48 hydrogen vehicles (HVs) are assumed for the 30-floor residential building with 480 households of 1440 residents based on a local survey showing that the car owner ratio in public housing of Hong Kong is about 9.9% [39]. The hydrogen vehicle model is developed from a commercialized product "2019 Toyota Mirai" with the maximum power output of 114 kW and maximum hydrogen storage tank mass of 5 kg at a maximum pressure of 700 bars. It is tested that the "Toyota Mirai" with full hydrogen storage can cover a cruise range of about 502 km [40]. 48 HVs are divided equally into two groups: the business worker group (group 1) and homemaker group (group 2) in different driving schedules. The average daily driving distances of the business worker and homemaker group are about 53.45 km and 36.75 km respectively [41], and the daily leaving home periods of these two groups are 8:00 - 19:00 on weekdays and 8:00 - 12:00 on every day respectively. HVs can meet the building load by consuming hydrogen in PEMFC when they are parked at home. The hydrogen consumption of HVs on the road is calculated but the detailed operation of HVs during the cruise is not the main focus of this study. Thermal heat is recovered from the electrolyzers, compressors and PEMFCs when HVs are parked at home to meet the air-conditioning reheat and domestic hot water demand of the building, thereby increasing the overall hydrogen system efficiency.

The hydrogen energy storage system consists of electrolyzers, compressor (*Com-t*) transporting hydrogen from the electrolyzers to a stationary hydrogen (H_2) storage tank (*Tank-st*) installed in the building, and two groups of hydrogen vehicles (*HV-g1*, *HV-g2*). A mobile H_2 storage tank (*Tank-g1*, *Tank-g2*) and proton exchange membrane fuel cell (*PEMFC-g1*, *PEMFC-g2*) are included in each HV, and a compressor (*Com-g1, Com-g2*) is allocated to each vehicle group to convey hydrogen from the stationary H_2 storage tank to each mobile H_2 tank when parked at home. The electrolyzer is modelled by TRNSYS Type 160a based on the advanced alkaline electrolyzer Phoebus [42]. The cell number varies in different cases based on the supply power entering the electrolyzer to keep the current density between 40 - 400 mA/cm^2 [43]. TRNSYS Type 167 is adopted to model the multistage compressor, which is turned on when the pressure of

entering hydrogen is lower than that of the targeted storage tank. The H_2 storage tanks are simulated by Type 164b to store compressed hydrogen at a high efficiency of around 99% with a maximum pressure of 700 bars based on the van der Waals equation of state for real gas [6]. The fuel cell is simulated by Type 170d for PEMFC showing the electrochemical process of converting the chemical energy of hydrogen and oxygen to electrical currents. The hydrogen storage tanks of HVs are checked over the night on each travelling day (0:00 - 8:00) and the utility grid feed the electrolyzer to generate hydrogen to secure the minimum FSOC level of mobile tanks for one-day cruise. The volume of the stationary H_2 storage tank needs to be optimized for system sizing as per Section 2.2.

***Energy management strategy* (*EMS*)**: Two energy management strategies with different operation priorities of the storage technologies are studied as the charging and discharging order of the battery tank and hydrogen vehicle has a significant impact on the technical and economic performance of the system. EMS 1 prioritizes battery storage over hydrogen storage when charging by surplus renewable energy or discharging for unsatisfied load, while EMS 2 performs in a reversed priority. Detailed control logics of EMS 1 and EMS 2 are illustrated in Fig. 5. Specifically, the available renewable power (P_{RE}) from PV panels and wind turbines is first used to meet the electrical load (P_{Load}) in the building under both strategies. In EMS 1, surplus renewable energy is controlled to charge the battery considering its maximum charging rate and available charging state as calculated by P_{Bat_charge}. Then, remaining renewable energy is used to drive the electrolyzer to generate hydrogen and store it in the stationary H_2 storage tank via the compressor (Com_t) according to its fractional state of charge ($FSOC_{st}$) which is also limited by the rated power of the electrolyzer (P_{Ele_rated}). The residual renewable energy is lastly fed into the utility grid when both the battery and H_2 storage tank are fully charged. The battery is operated to meet the load when renewable energy is not enough for the building demand, and its operation is limited by the maximum discharging rate and accessible discharging state of the battery as calculated by $P_{Bat\_discharge}$. The unmet load (P_{Load_req}) then needs to be covered by HVs parked at home with available hydrogen. Finally, the utility grid meets the remaining electrical load. While in EMS 2, the electrolyzer is charged by surplus renewable energy prior to the battery and HVs are discharged to meet the electrical demand before the battery. The selection signal of these two EMSs is set as one concerned variables in the multi-objective optimizations to determine the optimum EMS for

major stakeholders (i.e. the end-user, transmission system operator and investor) with different preferences.

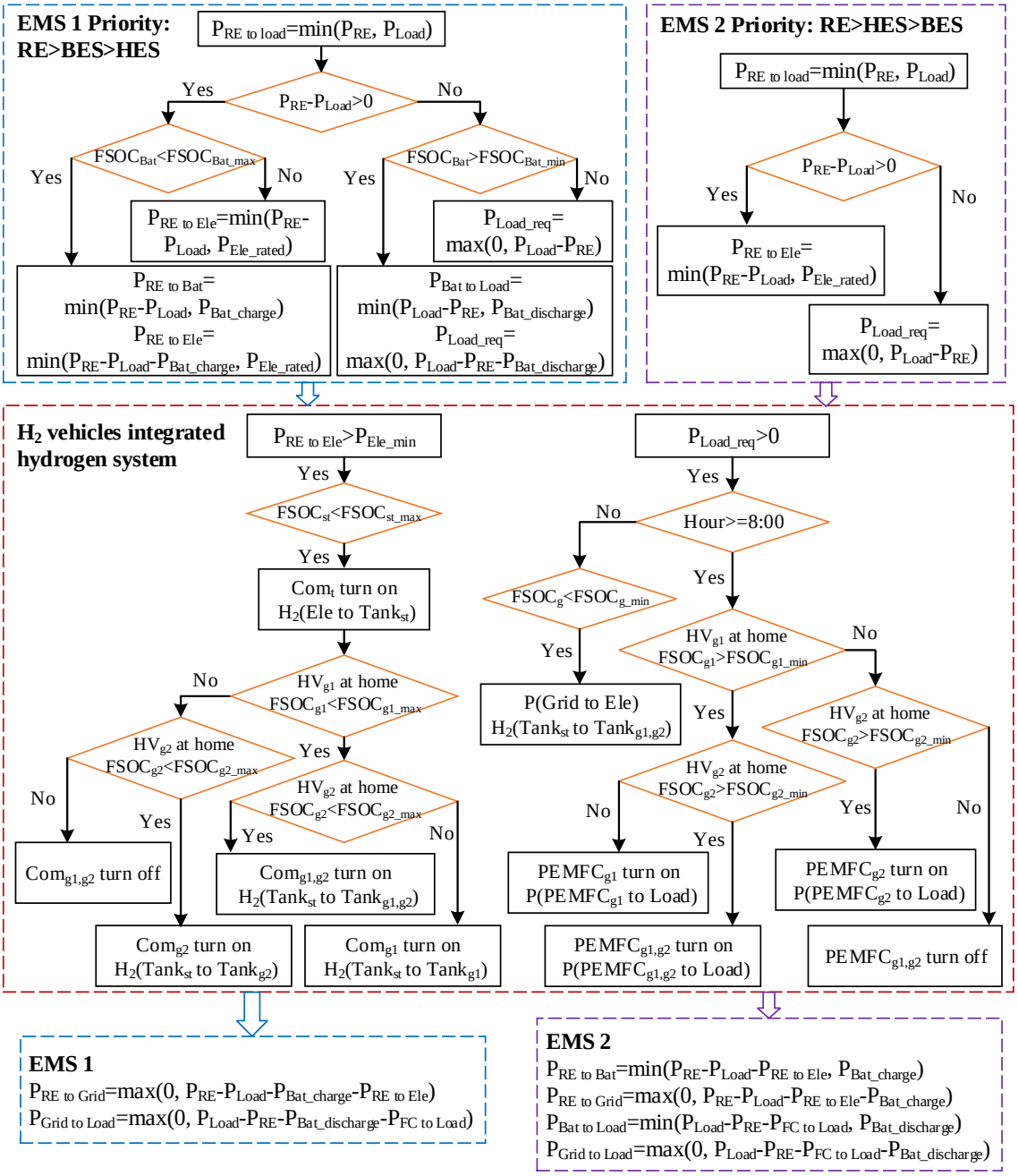

Fig. 5 Flow chart of hybrid PV-wind-battery-hydrogen system under two management strategies

The operation of the hydrogen energy storage system is determined by the two groups of HVs with different driving schedules. Compressed hydrogen is supplied from the stationary H_2 storage tank (*Tank*$_{st}$) to the mobile H_2 storage tanks of HVs parking at home according to the storage FSOC.

Specifically, available hydrogen is delivered from $Tank_{st}$ to the mobile tanks of HVs in group 1 ($Tank_{g1}$) via the compressor of group 1 (Com_{g1}) or to those of HVs in group 2 ($Tank_{g2}$) via the compressor of group 2 (Com_{g2}) when only one group of mobile tanks can be charged (the other group is either not at home or fully charged even though at home). And hydrogen in $Tank_{st}$ is equally supplied into $Tank_{g1}$ and $Tank_{g2}$ when both HV groups are parked at home with H_2 storage FSOC values lower than the maximum (0.95). HVs are operated to consume hydrogen in PEMFC to discharge power for the unmet electrical load when parked at home excluding the night time with a low electrical demand (0:00 - 8:00). Namely, the PEMFC of HVs parked at home in group 1 ($PEMFC_{g1}$) and group 2 ($PEMFC_{g2}$) is turned on when its H_2 storage tank FSOC is larger than its minimum to cover the one-day cruise (0.10647 in group 1, 0.07321 in group 2) and stay above the atmospheric pressure level (0.0024). During the night time period, the utility grid supplies power to drive the electrolyzer and charge H_2 storage tanks of HVs to secure its minimum FSOC level ($FSOC_{g1\_min}$ 0.10887, $FSOC_{g2\_min}$ 0.07561) for daytime travelling needs. The detailed design and operation parameters of the hybrid PV-wind-battery-hydrogen system are shown in Table 2. The initial cost of the PV and wind turbine is 3500 US$/kW and 4000 US$/kW respectively including installation investment with the same lifetime of 20 years [44]. The battery costs 1000 US$/kWh with a 5-year lifetime and the inverter costs 700 US$/kW with a 10-year lifetime [44]. The initial cost of the electrolyzer and compressor is 1400 US$/kW [6] and 15000 US$/Set [45] respectively. The H_2 storage tank costs 50 US$/N m^3 [46] and the HV costs 58500 US$ according to the official report of the manufacturer [47].

Table 2 Design and operation parameters of the hybrid PV-wind-battery-hydrogen system

Components	Initial cost	O&M ratio (of initial cost)	Lifetime, year
PV [44]	3500 US$/kW	2%	20
Wind turbine [44]	4000 US$/kW	1%	20
Battery [44]	1000 US$/kWh	1%	5
Inverter/converter [44]	700 US$/kW	1%	10
Electrolyzer	1400 US$/kW [6]	2% [46]	20 [48]
Compressor	15000 US$/Set [18]	2% [45]	20 [49]
H_2 storage tank [46]	50 US$/N m^3	0.50%	25
HV [47]	58500 US$/HV	2%	8

2.2. Design optimization of the hybrid PV-wind-battery-hydrogen system

2.2.1. Optimization methods and design variables

The multi-objective optimization is conducted using Non-dominated Sorting Genetic Algorithm II (NSGA-II) based on the joint platform of TRNSYS and jEplus+EA [50]. For NSGA-II applications, a higher crossover rate (0.9) is selected so that offspring solutions are closer to parent solutions, while a low mutation rate (0.05) is selected to maintain the convergence speed within a reasonable space [51]. The parent and offspring generations are combined to form the next-generation population with all solutions sorted into amounts of non-dominated fronts. The tournament selection between all solutions is then adopted to find the optimal front as the Pareto front [52]. The population size and maximum generation are set as 10 and 200 respectively to secure the search of global optima [53].

Four sizing variables are selected as design parameters of the hybrid PV-wind-battery-hydrogen system including the façade PV area, wind turbine number, battery capacity and stationary H_2 storage tank volume. The searching space of the installed façade PV area is 300 - 3900 m^2 at an increment of 600 m^2 which are installed on three façade areas (South, East and West) of the residential building with an adjacent shading factor of 76.64% [35]. The wind turbine number changes between 1 - 10 with a single turbine capacity of 100 kW and a power transmission loss of 13.541% [37]. The battery capacity is optimized between 240 - 2400 kWh (8 - 80 kWh/floor) at an interval of 240 kWh. The stationary H_2 storage tank volume of the hydrogen storage system is optimized within the range of 1 - 6 m^3 as the electrolyzer cell size is determined by the entering power supply to ensure the current density between 40 - 400 mA/cm^2 [43]. The selection signal of two developed EMSs is also set as an optimization variable for the optimum technical and economic performance of the hybrid renewable energy and storage system.

2.2.2. Formulation of optimization criteria

Both technical and economic performances of the hybrid PV-wind-battery-hydrogen system are evaluated with the multi-objective optimization. Below optimization criteria of the hybrid system comprehensively cover the main concerns of three key stakeholders: the end-user, transmission system operator and investor.

(1) System end-user

The end-user of the hybrid renewable energy and storage system concerns more about the supply performance which is expressed by a combined criterion integrating the self-consumption ratio of renewable energy, load cover ratio of the electrical demand and overall efficiency of the vehicle-integrated hydrogen storage system as shown in Eqs. (1) - (3).

Self-consumption ratio (*SCR*) of renewable sources:

$$SCR = \frac{on\text{-}site\ RE\ consumption}{total\ RE\ generation} = \frac{E_{RE\ to\ load} + E_{RE\ to\ battery} + E_{RE\ to\ electro}}{E_{RE}} \quad (1)$$

where $E_{RE\ to\ load}$ is the supplied PV and wind energy to the electrical load, kWh. $E_{RE\ to\ battery}$ is the charging energy from PV and wind sources to the battery, kWh. $E_{RE\ to\ electro}$ is the provided energy from PV and wind generation to the electrolyzer, kWh. E_{RE} is the total energy generation of PV panels and wind turbines, kWh.

Load cover ratio (*LCR*) of the electrical load:

$$LCR = \frac{on\text{-}site\ supply}{total\ electrical\ load} = \frac{E_{RE\ to\ load} + E_{battery\ to\ load} + E_{FCs\ to\ load}}{E_{load}} \quad (2)$$

where $E_{battery\ to\ load}$ is the discharging energy from the battery to the electrical load, kWh. $E_{FCs\ to\ battery}$ is the energy from fuel cells of HVs to the electrical load, kWh. E_{load} is the total electrical load covering the building load, electrical demand of the auxiliary electric heater and energy consumption for hydrogen compression, kWh.

Hydrogen system efficiency (*HSE*) with integrated hydrogen vehicles:

$$HSE = \frac{H_2\ system\ supply}{H_2\ system\ consumption} = \frac{E_{FCs\ to\ road} + E_{FCs\ to\ load} + E_{HR\ to\ reheat} + E_{HR\ to\ DHW}}{E_{RE\ to\ electro} + E_{grid\ to\ electro} + E_{comp} + E_{H_2\ tank}} \quad (3)$$

where $E_{FCs\ to\ road}$ is the energy from fuel cells to drive the motor of HVs when travelling, kWh. $E_{FCs\ to\ load}$ is the energy from fuel cells to cover the electrical load when HVs are parked at home, kWh. $E_{HR\ to\ reheat}$ is the heat recovered from the hydrogen system to meet the air-conditioning reheat demand, kWh. $E_{HR\ to\ DHW}$ is the heat recovered from the hydrogen system to meet the domestic hot water (DHW) load, kWh. $E_{grid\ to\ electro}$ is the refueled energy from the utility grid to drive the electrolyzer to generate hydrogen for HVs' daily cruise when FSOCs of H_2 storage tanks in HVs are lower than minimum thresholds, kWh. E_{comp} is the energy consumption of compressors in the

hydrogen system, kWh. $E_{H2\ tank}$ is energy change of the H_2 storage tanks during the evaluation period, kWh.

The end-user mainly concerns about the overall performance of the power supply (*Supply*) of the hybrid system by integrating three normalized indictors as shown in Eq. (4).

$$Supply = SCR_{nor} + LCR_{nor} + HSE_{nor} \quad (4)$$

where SCR_{nor} is the normalized value of self-consumption ratio. LCR_{nor} is the normalized value of load cover ratio and HSE_{nor} is the normalized value of hydrogen system efficiency. Normalization of these indicators is conducted as per Eq. (11).

(2) Transmission system operator

The hybrid renewable energy and storage system exchanges power with the utility grid by exporting surplus renewable energy and importing power for unmet demands, imposing great burden on the power transmission system in long-term and large-scale operations. It is therefore significant to control and optimize the grid integration for the hybrid system. The absolute net power exchange between the utility grid and hybrid system (See Eq. (5)) is developed as a decision-making reference for the transmission system operator.

$$NGE = ABS(grid\ supply - grid\ feed\text{-}in) = ABS(E_{grid\ to\ load} + E_{grid\ to\ electro} - E_{RE\ to\ grid}) \quad (5)$$

where *NGE* is the absolute value (ABS) of the difference in grid supply and grid feed-in energy, kWh. $E_{RE\ to\ grid}$ is the surplus energy from PV and wind sources to the utility grid, kWh.

(3) System investor

The net present value (*NPV*) is the difference between the present value of cash outflow and cash inflow of the hybrid system paid by the system investor as per Eq. (6).

$$NPV = PRV_{costs} - PRV_{FiT} \quad (6)$$

where PRV_{costs} is the present value of total costs of the system as formulated in Eq. (7) including the present value of the initial cost (PRV_{ini}), present value of the operation and maintenance cost ($PRV_{O\&M}$), present value of the replacement cost (PRV_{rep}) and present value of the residual cost (PRV_{res}), US$. PRV_{FiT} is the present value of the feed-in tariff (FiT) obtained by renewable energy generation according to the local FiT scheme, US$.

$$PRV_{costs} = PRV_{ini} + PRV_{O\&M} + PRV_{rep} - PRV_{res}$$

$$= C_{ini} + \sum_{n=1}^{n=N} \frac{f_{mai} \cdot C_{ini}}{(1+i)^n} + \sum_{j=1}^{j=J} C_{ini} \left(\frac{1-d}{1+i}\right)^{j \cdot l} - C_{ini} \frac{l_{res}}{l} \cdot \frac{(1-d)^N}{(1+i)^N} \quad (7)$$

where C_{ini} is the initial cost of system components including PV panels, wind turbines, batteries, inverters, electrolyzers, H_2 compressors, H_2 storage tanks and HVs, US$. n is a certain year and N is the lifetime of the hybrid system (20 years). f_{mai} is the ratio of the operation and maintenance cost to the initial cost. i is the annual real discount rate. j is the replace number of a specific component and J is the total replacement number. l_{res} is the residual lifetime and l is the lifetime of the component.

Renewable energy applications in Hong Kong can get a favorable amount of FiT subsidy at 3 HK$/kWh for a 200 - 1000 kW system until end 2033, while the renewable generation thereafter will be owned by the system investor. It can then be assumed that FiT subsidy after 2033 can be obtained at the rate of the local electricity price for renewable generation as shown in Eq. (8).

$$PRV_{FiT} = \sum_{n=1}^{n=13} \frac{\left(E_{PV} \cdot (1-\delta_{PV})^{n-1} + E_{WT} \cdot (1-\delta_{WT})^{n-1}\right) \cdot c_{fit}}{(1+i)^n} + \sum_{n=14}^{n=20} \frac{(E_{PV} \cdot (1-\delta_{PV})^{n-1} + E_{WT} \cdot (1-\delta_{WT})^{n-1}) \cdot c_{ele} \cdot (1+\gamma)^{n-1}}{(1+i)^n} \quad (8)$$

where E_{pv} is the energy generation of PV panels, kWh. δ_{PV} is the annual degradation rate of the PV system. E_{wt} is the energy generation of wind turbines, kWh. δ_{WT} is the annual degradation rate of the wind turbine system. c_{fit} is the feed-in tariff in the first 13 years issued by the government, US$/kWh. c_{ele} is the local electricity price of residential buildings, US$/kWh. And γ is the annual price increasing rate of the electricity. Detailed parameters for the economic assessment are shown in Table 3.

Table 3 Parameters of the hybrid PV-wind-battery-hydrogen system for the economic assessment

Parameter	Value
Real discount rate (i)	5.8%/year [54]
Feed-in tariff (c_{fit})	0.3846 US$/kWh [55]
Electricity tariff of residence (c_{ele})	0.145 US$/kWh [56]
Electricity tariff increasing rate (γ)	1.4%/year [57]
PV degradation rate (δ_{PV})	1%/year [58]
Adjacent shading factor of façade PV	76.64% [35]

Parameter	Value
Wind turbine degradation rate (δ_{WT})	1.5%/year [59]
Power transmission loss rate	13.541% [37]
Battery price degression rate	5%/year [60]
Inverter price degression rate	10.15%/year [61]
H_2 storage tank price degression rate	4.2%/year [62]
HV price degression rate	4.3%/year [63]
Carbon intensity of electricity	0.66 $kgCO_2$/kWh [64]

2.2.3. Multi-objective optimization decision-making strategy

Decision-making strategies (DMSs) are required to determine a final optimum solution out of the obtained Pareto optimal set. Four decision-making strategies are considered focusing on different concerns of major stakeholders of the hybrid system. The minimum distance to the utopia point method is adopted for DMS 1 with equivalent priority to all evaluated criteria. The analytical hierarchy process method is adopted for DMS 2: the end-user priority, DMS 3: the transmission system operator priority, and DMS 4: the investor priority.

(1) DMS 1 with the minimum distance to the utopia point (MDUP) method

The utopia point of the multi-objective optimization is an ideal optimum solution supposing all objectives to be minimized simultaneously. The MDUP method obtains the optimum solution by calculating the distance to the utopia point as the multi-objective optimization coefficient (MOOC) as per Eq. (9), whose minimum value is adopted to identify the final optimum solution [52]. An equivalent weighting is applied to all optimization objectives in the MDUP method.

$$MOOC = \|P_i - P_u\| \tag{9}$$

where P_i is the Pareto optimal solutions and P_u is the utopia point.

(2) DMSs 2 - 4 with the analytical hierarchy process (AHP) method

The AHP method obtains the weights of different optimization criteria via structuring a decision matrix $D_{m\times m}$ consisting of all concerned objectives with different levels of importance valued by decision-makers. A pairwise comparison among optimization criteria is established by defining D_{ij}, which is larger than 1 if objective i is prioritized over j ($D_{ji} = 1/D_{ij}$). D_{ij} is an integer

varying between 1 - 9 defined by Saaty showing that 1 means objective *i* and *j* is equally important and 9 means objective *i* is extremely important than *j* [65]. The consistency ratio of the decision matrix should be kept lower than 0.1 by calculating the principal eigenvalue to ensure the reasonability of the established matrix of optimization criteria [66]. The scale of weights can be then derived by solving and normalizing the principal eigenvector of the decision matrix. The AHP method is adopted to derive the weights of optimization objectives considering the preferences of three major stakeholders of the hybrid system. Specifically, the end-user of the hybrid system prioritizes the supply performance indicator integrating *SCR*, *LCR* and *HSE* (DMS 2). The transmission system operator values the grid integration most (DMS 3) while the investor's major concern is the net present cash flow (DMS 4). The decision matrix of DMSs 2 - 4 based on the AHP method is shown in Table 4.

Table 4 Decision matrix of DMSs 2 - 4 based on analytical hierarchy process method

DMS 2: End-user priority				DMS 3: Transmission system operator priority				DMS 4: Investor priority			
	Supply	*NGE*	*NPV*		*Supply*	*NGE*	*NPV*		*Supply*	*NGE*	*NPV*
Supply	1	9	5	*Supply*	1	1/5	2	*Supply*	1	2	1/5
NGE	1/9	1	1/2	*NGE*	5	1	9	*NGE*	1/2	1	1/9
NPV	1/5	2	1	*NPV*	1/2	1/9	1	*NPV*	5	9	1
Weight	0.761	0.082	0.158	Weight	0.158	0.761	0.082	Weight	0.158	0.082	0.761
consistency ratio=0.1%				consistency ratio=0.1%				consistency ratio=0.1%			

The evaluating criterion (i.e. MOOC) to select a final optimum solution out of the Pareto solutions with the AHP method is shown in Eq. (10).

$$MOOC = WT_{Supply} \cdot Supply_{nor} + WT_{NGE} \cdot NGE_{nor} + WT_{NPV} \cdot NPV_{nor} \tag{10}$$

where WT_{Supply}, WT_{NGE}, WT_{NPV} are the weights of optimization objectives *Supply*, *NGE* and *NPV* obtained by the decision matrix. $Supply_{nor}$, NGE_{nor}, NPV_{nor} are the normalized values of optimization criteria *Supply*, *NGE* and *NPV* as per Eq. (11) [67].

$$Obj_{nor} = \frac{Obj_i - Obj_{min}}{Obj_{max} - Obj_{min}} \tag{11}$$

where Obj_{nor} is the normalized value of optimization objectives *Supply*, *NGE* and *NPV*. Obj_i is the original value of the optimization objective. Obj_{min} and Obj_{max} are the minimum and maximum values of corresponding objectives.

3. Results and discussion

3.1. Design optimization results of the hybrid renewable energy and storage system

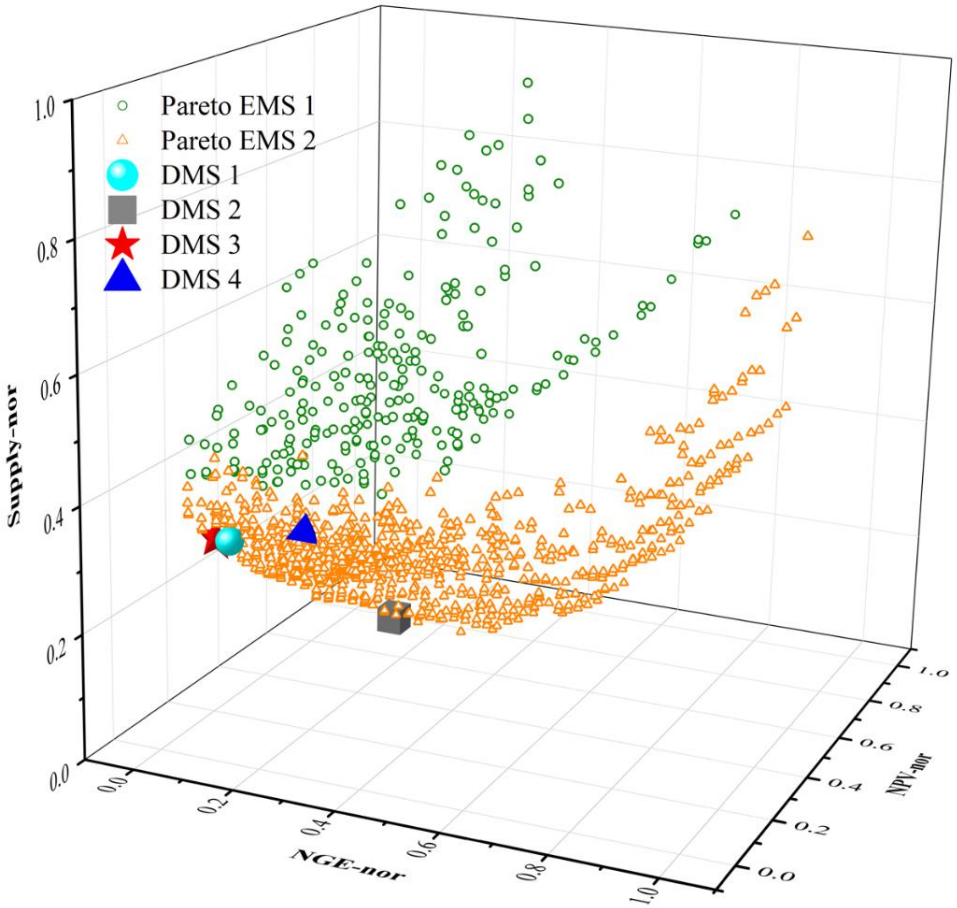

Fig. 6 Pareto optimal and final optimum results of four decision-making strategies

The Pareto optimal solutions are obtained through the multi-criterion optimizations by varying the EMS selection and system sizing variables for techno-economic indicators of the hybrid PV-wind-battery-hydrogen system including *SCR*, *LCR*, *HSE*, *NGE* and *NPV*. These best solutions are then normalized as per Eq. (11) and the supply performance indicators (i.e. *SCR*, *LCR* and *HSE*) are combined according to Eq. (4) with the weighted sum method as an integrated objective *Supply*. The three-dimensional Pareto optimal surface is then demonstrated in Fig. 6 consisting of three normalized objectives (i.e. *Supply*, *NGE* and *NPV*). It is indicated that both

EMS 1 (BES prioritized over HES) and EMS 2 (HES prioritized over BES) are selected in the Pareto optimal set with different optimization focuses. Four DMSs based on MDUP and AHP are further adopted to select the final optimum solution out of the Pareto optimal solutions for key stakeholders. It is found that the optimum solutions of these four DMSs are achieved with EMS 2 where hydrogen storage is prioritized over battery storage.

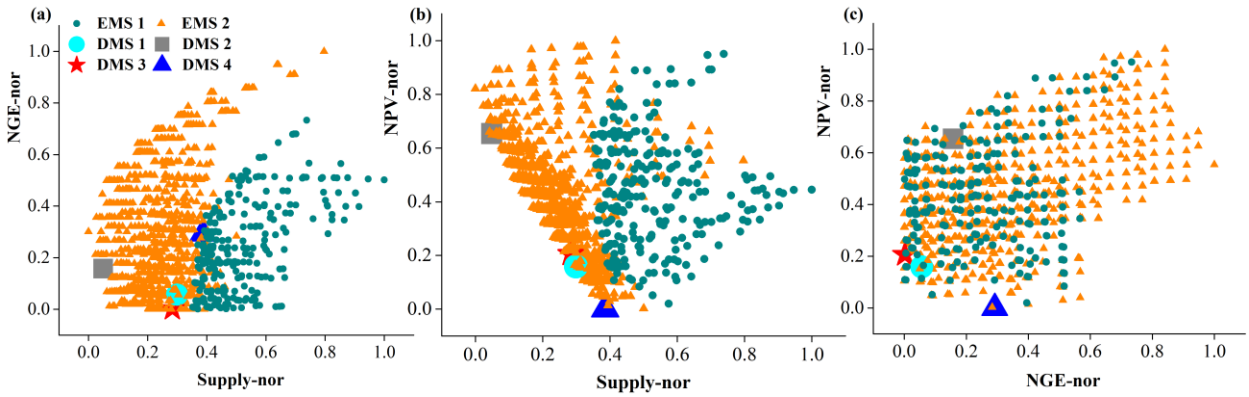

Fig. 7 Projection distribution of Pareto optimal and final optimum results

Fig. 7 shows the two-dimensional projection of Pareto optimal solutions of EMS 1 and EMS 2 with the highlighted final optimum solutions under four DMSs. It is found that EMS 2 dominates the best solution when considering objective combinations of *Supply-NGE* and *Supply-NPV* as per Fig. 7 (a, b), because the indicator *Supply* (integrating *SCR*, *LCR* and *HSE*) achieves better performance under EMS 2 where hydrogen storage is prioritized over battery storage. Namely, EMS 2 should be selected as the energy management scheme of the hybrid system when focusing on the system supply and grid integration or system supply and economy performance. However, no clear dominance is observed between EMS 1 and EMS 2 when considering the *NGE-NPV* objective combination as shown in Fig. 7 (c), because the change of EMSs with different operation priorities of storage has minor impact on the system *NGE* and *NPV*. It means that both EMS 1 and EMS 2 are applicable when focusing on the grid integration and system economy performance. The results of optimum solutions under four DMSs are shown in Table 5.

Table 5 Sizing results of four decision-making strategies for the hybrid system

Optimization results	Facade PV /m^2	Wind turbine number	Battery capacity /kWh	Stationary H_2 tank /m^3
Equivalent priority (DMS 1)	1500	8	480	5
End-user priority (DMS 2)	3900	5	1920	4
Transmission system operator priority (DMS 3)	900	8	720	5
Investor priority (DMS 4)	900	10	240	6

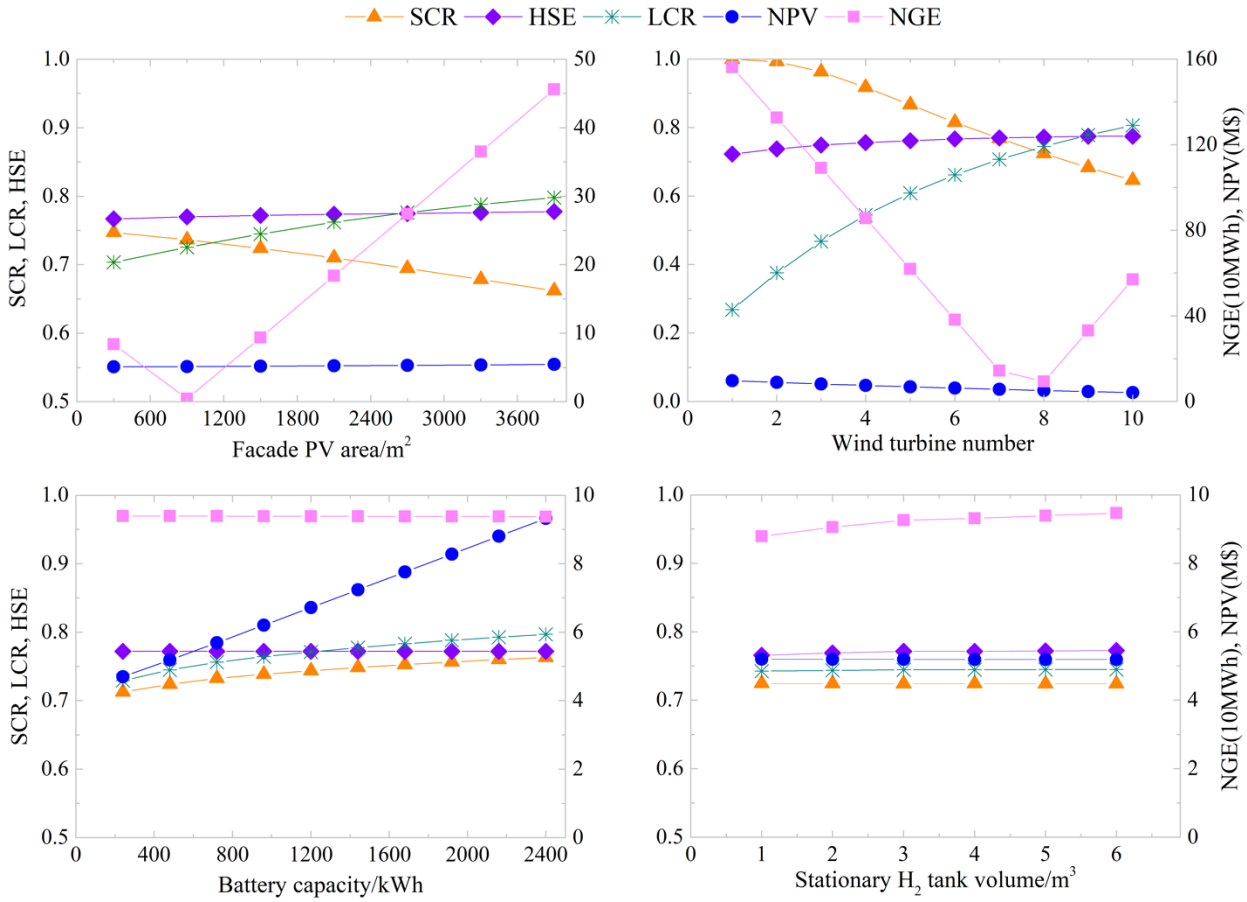

Fig. 8 Sensitivity analysis of design variables on optimization objectives of the hybrid system

The sensitivity analysis of four sizing variables for the optimization objectives of the hybrid system is shown in Fig. 8 with the optimum solution by DMS 1 as the baseline case. It is indicated

that *SCR* decreases with the rising façade PV area and wind turbine number given more available renewables power while *SCR* increases with the battery capacity for more on-site renewable energy consumption. The *HSE* improves with the rising PV and wind capacity due to more energy storage in the hydrogen system, and it is less sensitive to the changing battery capacity because hydrogen storage is prioritized over battery storage in EMS 2. The *LCR* shows a steady rise with the larger façade PV area, wind turbine number and battery capacity due to more available power supply from the hybrid system. And the *NPV* rises sharply with the increasing battery capacity as the initial cost of the battery is relatively high and subject to replacement every five years. The *NGE* shows a steady drop with the rising battery capacity as more grid exchange can be waived by batteries which can meet the electrical load and consume surplus renewable energy. The stationary H_2 tank volume imposes a relatively lower impact on the optimization objectives compared with the other design variables.

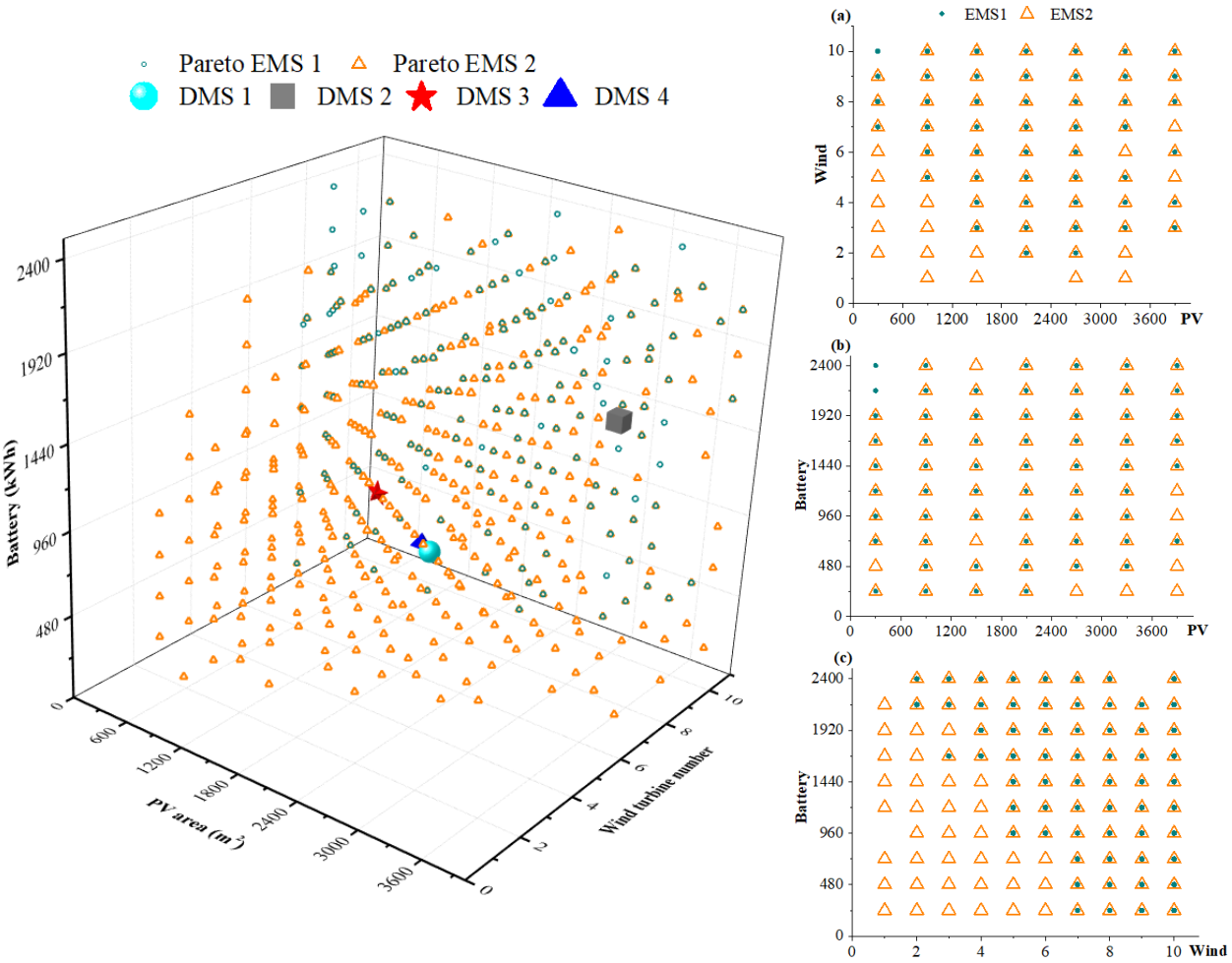

Fig. 9 Distribution of sizing variables of EMS 1 and EMS 2 of Pareto optimal solutions

Fig. 9 shows the distribution of sizing variables (i.e. the façade PV area, wind turbine number and battery capacity) in the Pareto optimal set of the hybrid system under EMS 1 and EMS 2. These three sizing variables are previously demonstrated to have a greater impact on the optimization objectives compared with the stationary H_2 tank volume (See Fig. 8). EMS 2 achieves better performance in terms of the supply performance (integrating *SCR*, *LCR* and *HSE*) compared with EMS 1, and these supply indicators are more sensitive to sizing variables at low magnitudes based on the previous sensitivity analysis. Therefore, the superiority of EMS 2 is more obvious in small-scale systems, while EMS 1 and EMS 2 are comparable in large-scale systems. In summary, EMS 2 has a wider applicability in the hybrid system with different PV, wind and battery capacities to achieve the optimum techno-economic performance (*Supply*, *NGE* and *NPV*). While EMS 1 is suitable for the hybrid system with large PV, wind and battery capacities in the multi-objective optimization.

3.2. Techno-economic-environmental analysis of optimum design solutions

(1) Technical analysis of the hybrid renewable energy and storage system

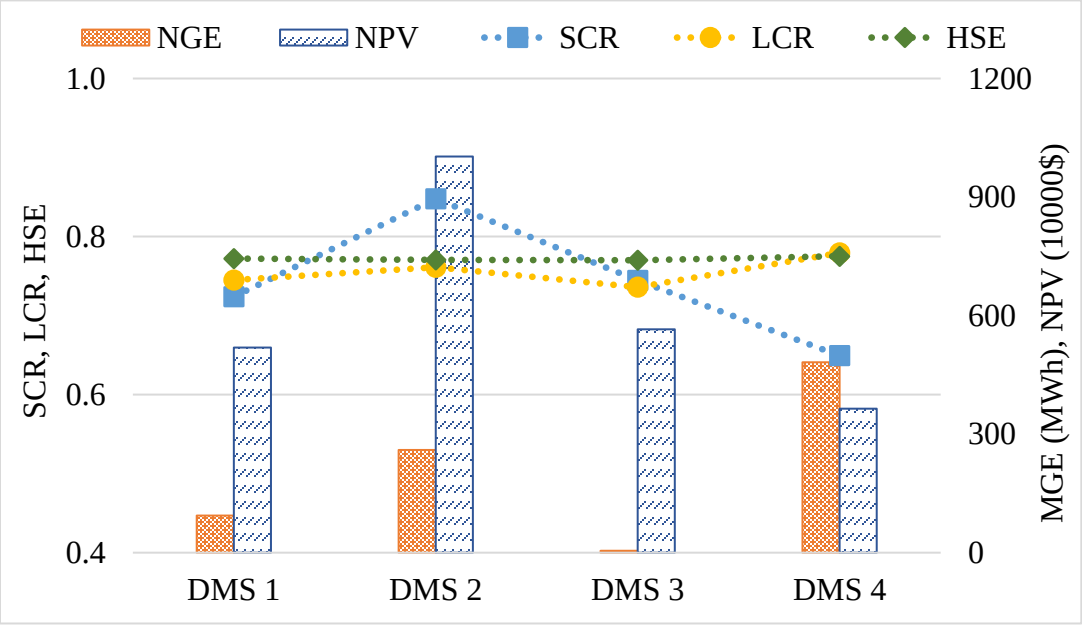

Fig. 10 Results of optimum solutions of four DMSs of the hybrid system

The optimum results of four DMSs of the hybrid system are compared in Fig. 10 including the annual average self-consumption of renewable energy (*SCR*), cover ratio of the electrical load

(*LCR*), overall efficiency of the hydrogen system (*HSE*), absolute value of the net grid exchange (*NGE*) and net present value (*NPV*). The annual average *SCR* reaches its maximum of 84.79% in DMS 2 with the minimum wind power generation and a relatively low *SCR* (64.93%) is observed in DMS 4 with the maximum wind power generation. The *LCR* shows a minor variation with the maximum of 77.93% under DMS 4. A relatively stable annual average *HSE* is observed among all DMSs between 77.00% - 77.52% as hydrogen storage is prioritized over battery storage for energy charging and discharging in EMS 2. Majority of released heat of the hydrogen system can be recovered to cover the air-conditioning reheat and domestic hot water demand in the building with the annual average heat recovery efficiency (*HRE*) between 95.17% - 95.46%. DMS 1 achieves a relative balance among all optimization objectives with an equivalent priority. DMS 2 (focusing on the end-user's concern) has the optimum performance on the integrated objective *Supply* with an annual average *SCR*, *LCR* and *HSE* of 84.79%, 76.11% and 77.06% respectively. DMS 3 (focusing on the transmission system operator's concern) has the minimum *NGE* of 4.55 MWh between the utility grid and the hybrid system compared to the maximum of 482.19 MWh in DMS 4 with the maximum wind energy and minimum battery capacity. DMS 4 (focusing on the investor's concern) achieves a minimum lifetime *NPV* of about 3.64 M$ with a detailed breakdown in the economic analysis.

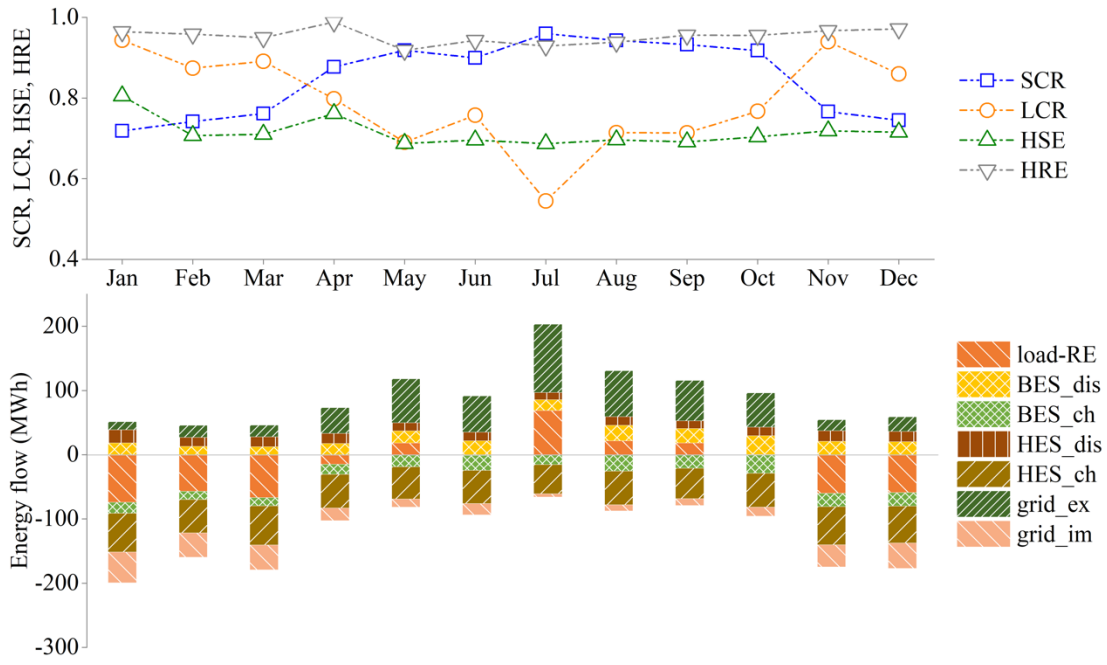

Fig. 11 Monthly energy flow and technical performance of the hybrid system in DMS 2

The monthly energy flow of major components in the hybrid system and important technical indicators are demonstrated for the final optimum solution of DMS 2 (i.e. supply performance prioritized) as per Fig. 11 (power out: positive; power in: negative). An obvious imbalance between the load and supply is observed with a large renewable energy surplus from November to March and unsatisfied electrical load in July. The charging and discharging energy of battery storage is relatively balanced, while charging energy of hydrogen storage is notably larger than the discharging energy to the electrical load due to the large consumption of HVs on road. The monthly average *SCR* firstly increases and then decreases peaking at 95.96% in July while the monthly average *LCR* shows a reversed trend with a maximum of 94.34% in January. The monthly *HSE* evaluating the energy storage and heat recovery also varies with the mismatch between the supply and demand at 68.67% - 80.51%. The majority of released heat from the hydrogen storage system can be recovered for the air-conditioning reheat and domestic hot water demand in the building with a monthly *HRE* between 91.81% - 98.82%. Over half of total annual electrical load is covered by on-site renewable energy from PV and wind sources, where battery storage and hydrogen storage undertake 13.86% and 10.34% respectively with the remaining 23.89% from the grid.

(2) Economic analysis of the hybrid renewable energy and storage system

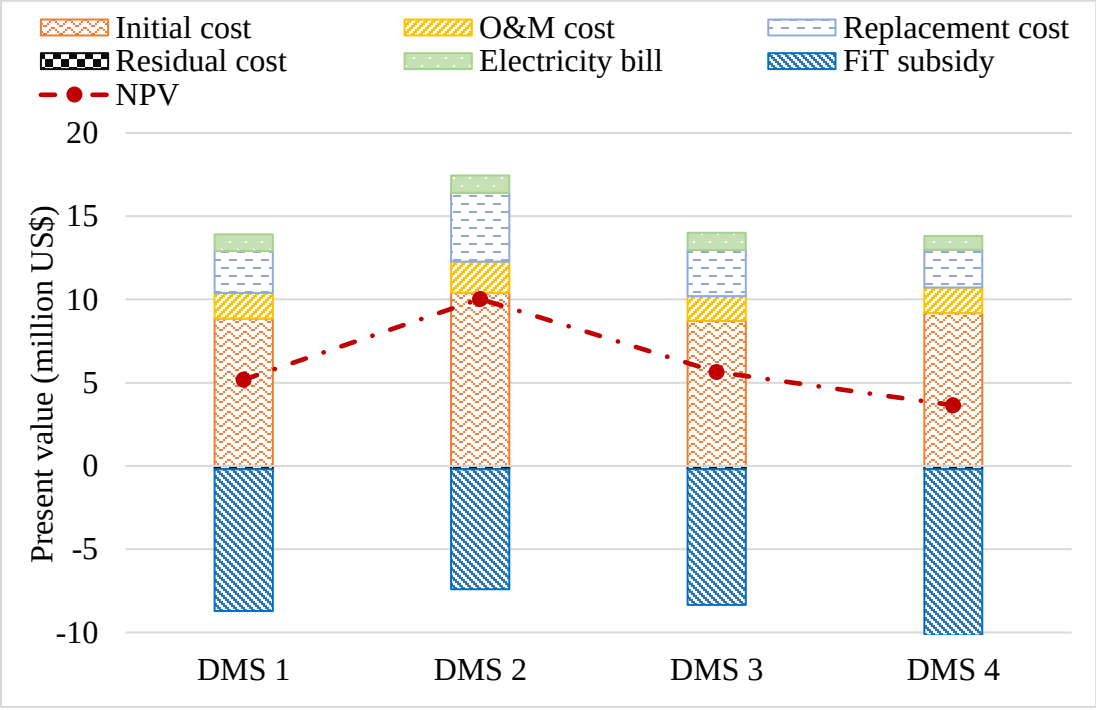

Fig. 12 Lifetime present value of four optimum cases of the hybrid system

Fig. 12 shows the detailed lifetime present value of the hybrid system under four DMSs. The highest investment cost of 16.40 M$ consisting of the initial cost, operation and maintenance cost (O&M cost) and replacement cost is derived from DMS 2 with the largest PV and battery capacity. The residual cost mainly from hydrogen storage tanks and HVs accounts for a relatively small proportion and shows a minor difference among all cases at about 0.19 M$. A large amount of FiT subsidy can be harvested by the investor in Hong Kong with a maximum of 9.99 M$ under DMS 4. The detailed breakdown of the *NPV* is shown in Table 6. It is indicated that the lifetime *NPV* under DMS 4 (investor priority) is the minimum among four DMSs as the economic performance is prioritized by the system investor. The annual electricity bill of DMS 4 is reduced by 15.44% compared with that of the equivalent priority case (DMS 1) and DMS 4 also gets the maximum amounts of annual FiT subsidy, 14.67% higher than that of DMS 1. The lifetime *NPV* of DMS 4 is about 3.64 M$, which is much lower than that of DMS 1 by 29.88%.

Table 6 Economic analysis of four optimum cases of the hybrid system

Economic analysis	DMS 1 (equivalent priority)	DMS 2 (end-user priority)	DMS 3 (transmission system operator priority)	DMS 4 (investor priority)
Initial cost, M$	8.85	10.39	8.71	9.17
O&M cost, M$	1.55	1.87	1.49	1.55
Replacement cost, M$	2.51	4.14	2.77	2.26
Residual cost, M$	-0.19	-0.19	-0.19	-0.19
Electricity bill, M$	1.00	1.04	1.03	0.84
FiT subsidy, M$	-8.52	-7.22	-8.17	-9.99
NPV, M$	5.19	10.03	5.65	3.64

The impact of the initial cost fluctuation of storage technologies (battery and electrolyzer) on the lifetime *NPV* of the hybrid system is further discussed. The initial cost of storage technologies is varied from a relatively high market price to a low market price. Specifically, the battery price varies from 1000 US$/kWh [44] to 580 US$/kWh according to an updated literature [68], and the electrolyzer price varies from 1400 US$/kW to 500 US$/kW as estimated by International Energy Agency [69]. The lifetime *NPV* variation on top of its optimum value under four DMSs is presented in Fig. 13. It is indicated that the *NPV* reduction magnitudes (409.55 k$) caused by the electrolyzer

price decrease are the same throughout four cases given the same calculated maximum electrolyzer cell numbers as determined by the entering power supply from renewable generation or utility grid. While the *NPV* reduction ratios of the four cases compared with the high market price scenario vary between 4.08% - 11.25%. The *NPV* magnitude is reduced by 6.20% - 18.01% among four cases when the battery price decreases to a low market level, with a maximum decline of 1806.26 k$ in DMS 2 (the maximum battery capacity scenario). It shows that the price fluctuation of storage technologies in the hybrid system has a significant contribution to reducing the lifetime *NPV*.

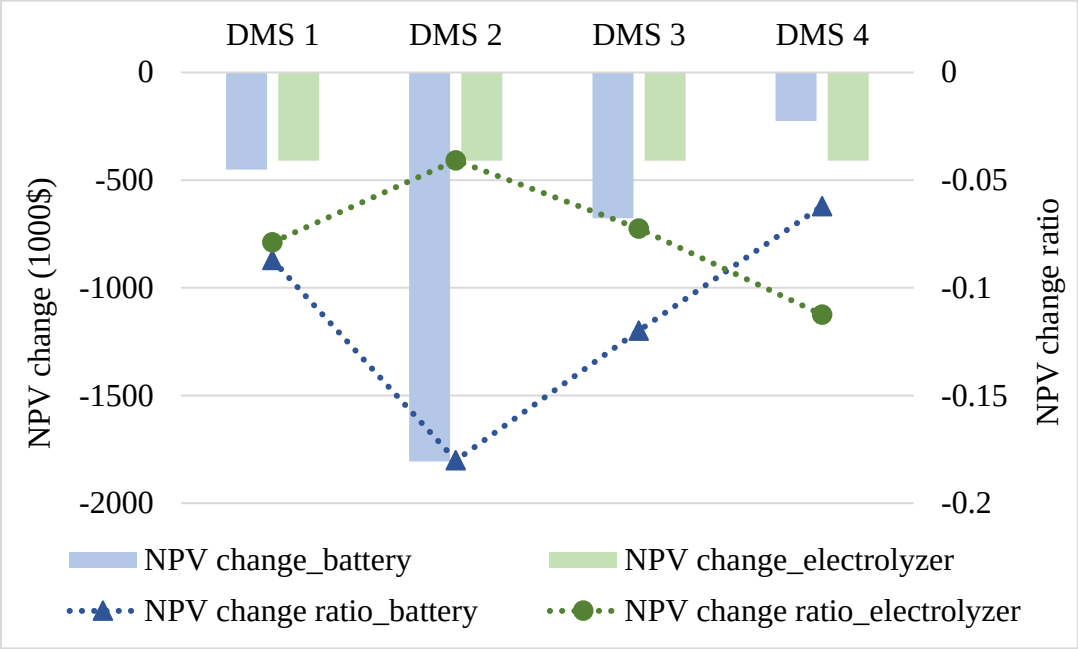

Fig. 13 Impact of storage technology prices on the system net present value

The impact of two important economic parameters (i.e. the HV lifetime and FiT mode) on the system *NPV* of four DMSs is further discussed in Fig. 14 (a, b). The system *NPV* decreases with the rising HV lifetime due to a lower cost of the hydrogen system. The system *NPV* is decreased by 13.49% - 37.16% among these four DMSs when the HV lifetime is changed from 8 years to 16 years. The current renewable energy FiT scheme in Hong Kong provides a subsidy of 3 HK$/kWh for a 200 - 1000 kW renewable system before 2033, while FiT subsidy after 2033 is not clearly specified. Therefore, three hypothetical FiT modes are discussed for system FiT after 2033: FiT mode 1 - an FiT rate of 3 HK$ for renewables generation in line with that before 2033; FiT mode 2 - an FiT rate at the local electricity rate for renewable generation as adopted in previous design optimizations; FiT mode 3 - an FiT rate at the local electricity rate for grid exported

renewable energy. The system *NPV* is decreased by 8.92% - 33.52% when the FiT mode is changed from mode 2 to mode 1 following a higher subsidy rate. And a remarkable increase of 61.59% - 182.96% in the system *NPV* is observed when the FiT mode is changed from mode 2 to mode 3 with less counted renewable generation.

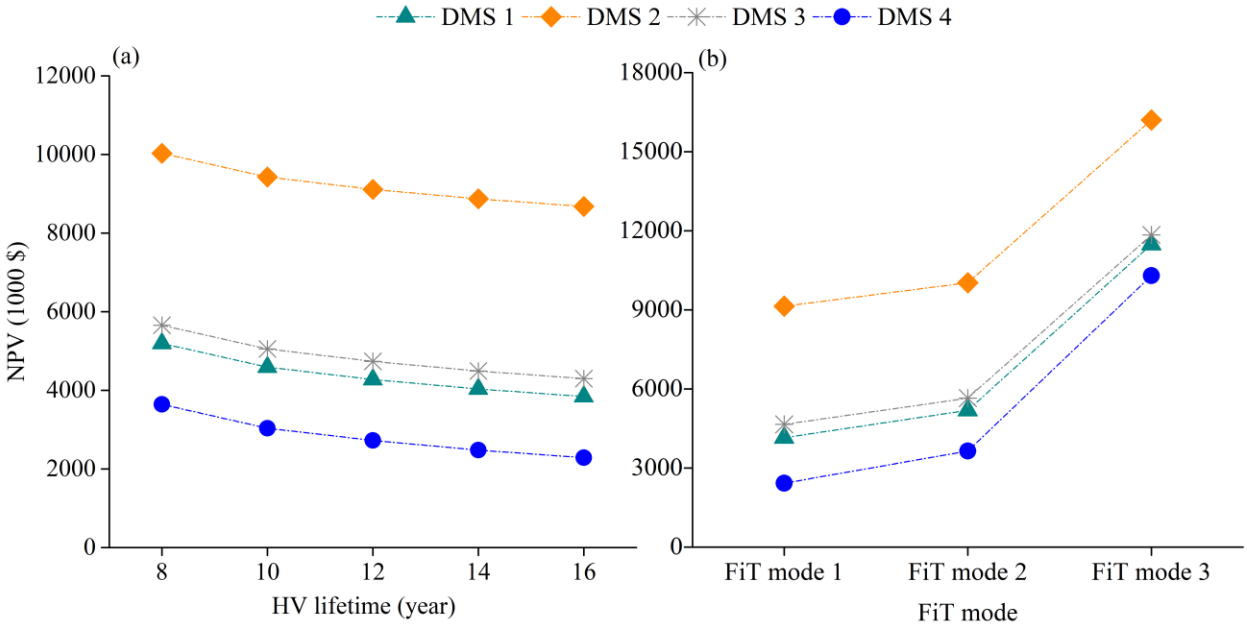

Fig. 14 Impact of HV lifetime and FiT mode on the system net present value

(3) Environmental analysis of the hybrid renewable energy and storage system

The monthly carbon emissions of optimum solutions for the hybrid system are determined by the grid imported energy and renewable energy generation as per Fig. 15 [54], considering a power transmission loss rate of 0.13541 [37] and local carbon intensity of 0.66 $kgCO_2/kWh$ [64]. The carbon emission can be negative indicating more renewable generation than grid import, or zero indicating carbon neutrality for power supply to the high-rise building. The carbon emission in July under DMS 3 is positive showing that more power needs to be supplied from the utility grid compared with the generated renewable energy in a high electrical load condition. And the carbon emissions in other months are all negative with a positive impact on the sustainable environment development. The total annual carbon emissions of all four cases are negative with the minimum of -196.82 tCO_2 under DMS 4, indicating that environmental benefits can be achieved together with economic profits.

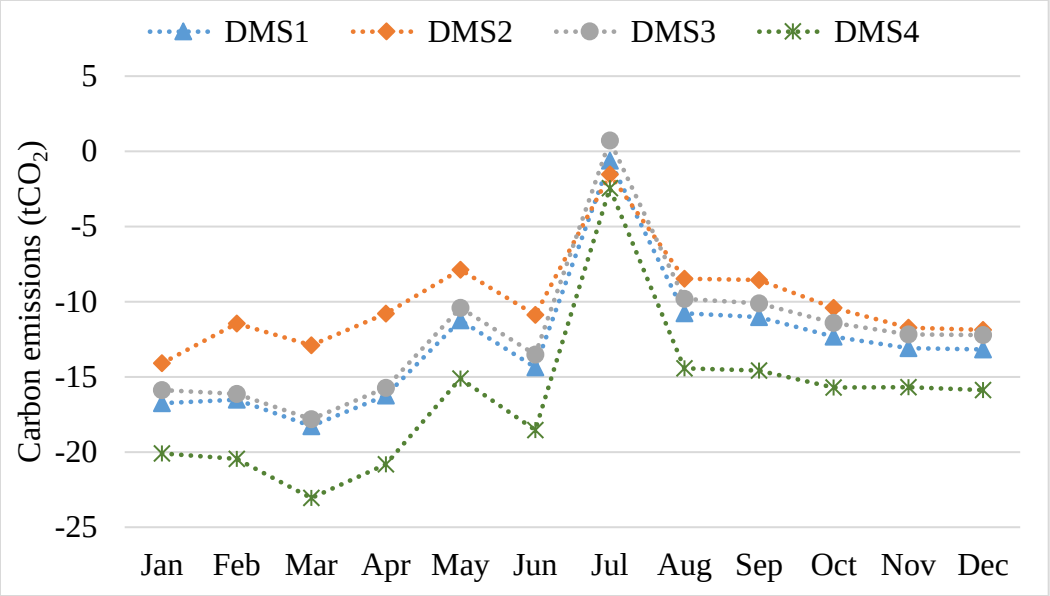

Fig. 15 Monthly carbon emissions of four DMSs of the hybrid system

4. Conclusions

This study comprehensively analyzes techno-economic-environmental performances of hybrid photovoltaic-wind-battery-hydrogen systems for power supply to typical high-rise residential buildings with a robust multi-objective design optimization and parametric analysis approach. Two energy management strategies with different priorities of battery and hydrogen storage operations are developed and four decision-making strategies reflecting different stakeholders' concerns are applied to explore the final optimum solutions. Important conclusions are summarized as below:

(1) Two energy management strategies are proposed for the hybrid system with stationary battery storage and two groups of mobile hydrogen vehicles following different cruise schedules, and subject to multi-objective optimizations together with other design variables for a typical high-rise residential building.

(2) It is suggested that both energy management strategy 1 (with battery storage prioritized over hydrogen storage) and energy management strategy 2 (with reversed priority) are suitable for optimizing the grid integration-system economy performance. The Energy Management Strategy 2 should be selected when focusing on the system supply-grid integration or system supply-economy performance. It is also indicated that the Energy Management Strategy 2 has a wider

range of applicability in hybrid systems with different photovoltaic, wind and battery installation capacities to achieve the optimum techno-economic performance considering system supply, grid integration and economic indicators. While the Energy Management Strategy 1 is suitable for hybrid systems with large photovoltaic, wind and battery installation capacities in the techno-economic optimization.

(3) The equivalent priority case (Decision-making Strategy 1) can achieve a relatively balanced results among all the optimization objectives while Decision-making Strategy 2 focusing on the concern of end-users has the optimum supply performance with an annual average self-consumption ratio, load cover ratio and hydrogen system efficiency of 84.79%, 76.11% and 77.06%, respectively. Decision-making Strategy 3 prioritizes the grid integration performance for the transmission system operator and thus has the minimum absolute net grid exchange of 4.55 MWh, much lower than the maximum of 482.19 MWh in Decision-making Strategy 4. Majority of released heat from the hydrogen system can be recovered to meet the air-conditioning reheat and domestic hot water demand in the building with an annual average heat recovery efficiency between 95.17% - 95.46% across the four optimum cases.

(4) The system lifetime net present value of the investor priority case (Decision-making Strategy 4) is the most favorable with the minimum electricity bill and maximum feed-in tariff subsidy of about 3.64 M$, much lower than that in the equivalent priority case (Decision-making Strategy 1) by 29.88%. The price fluctuation of battery storage and hydrogen storage technologies from high market to low market price scenarios has a significant impact on reducing the system lifetime net present value. A reduction of 4.08% - 11.25% and 6.20% - 18.01% is derived from the electrolyzer and battery respectively among four decision-making strategies. The system net present value is decreased by 13.49% - 37.16% among four decision-making strategies when the hydrogen vehicle lifetime is changed from 8 years to 16 years. A remarkable impact of the feed-in tariff mode on the system net present value is also observed with an 8.92% - 33.52% decrease from mode 2 to mode 1 and 61.59% - 182.96% increase from mode 2 to mode 3. The four optimum cases can also achieve negative total annual carbon emissions showing a positive impact on the sustainable environmental development. Especially, the minimum annual carbon emission of -196.82 tCO_2 is obtained from the investor priority case (Decision-making Strategy 4).

(5) This design optimization study on hybrid photovoltaic-wind-battery-hydrogen systems for power supply to typical high-rise residential buildings integrated with hydrogen vehicles provides optimal sizing configurations and energy management schemes for major stakeholders with different concerns. The detailed and in-depth technical, economic and environmental performance analysis offers valuable references for energy planning of hybrid renewable energy and storage systems for future large-scale building applications in high-density urbanized regions.

Nomenclature

Acronyms

AHP:	analytical hierarchy process
BES:	battery energy storage
DHW:	domestic hot water
DMS:	decision-making strategy
EMS:	energy management strategy
FiT:	feed-in tariff
FSOC:	fractional state of charge
HES:	hydrogen energy storage
HSE:	hydrogen system efficiency
HV:	hydrogen vehicle
LCR:	load cover ratio
MDUP:	minimum distance to the utopia point
MOOC:	multi-objective optimization criterion
NGE:	absolute value of net grid exchange
NPV:	net present value
PEMFC:	proton exchange membrane fuel cell
PV:	photovoltaic
RE:	renewable energy
SCR:	self-consumption ratio
WT:	wind turbine

List of symbols

c_{ele}:	local electricity price, US$/kWh
c_{fit}:	feed-in tariff, US$/kWh
C_{ini}:	initial cost, US$
$E_{battery\ to\ load}$:	energy from battery to electrical load, kWh
E_{comp}:	energy consumption of compressors, kWh
$E_{FCs\ to\ battery}$:	energy from fuel cells to electrical load, kWh

$E_{FCs\ to\ load}$: energy from fuel cells to electrical load, kWh

$E_{FCs\ to\ road}$: energy from fuel cells to hydrogen vehicles used on the road, kWh

$E_{grid\ to\ electro}$: energy from grid to electrolyzer, kWh

$E_{HR\ to\ DHW}$: heat recovery of hydrogen system to meet domestic hot water load, kWh

$E_{HR\ to\ reheat}$: heat recovery of hydrogen system to meet air-conditioning reheat load, kWh

$E_{H2\ tank}$: energy change of hydrogen storage tanks, kWh

E_{load}: total electrical load, kWh

E_{pv}: energy generation of PV panels, kWh

E_{RE}: renewable energy generation, kWh

$E_{RE\ to\ battery}$: energy from renewable energy to battery, kWh

$E_{RE\ to\ electro}$: energy from renewable energy to electrolyzer, kWh

$E_{RE\ to\ grid}$: energy from renewable energy to grid, kWh

$E_{RE\ to\ load}$: energy from renewable energy to electrical load, kWh

E_{wt}: energy generation of wind turbines, kWh

f_{mai}: ratio of operation and maintenance cost to initial cost

$FSOC_{Bat\_min}$: minimum value of battery fractional state of charge

$FSOC_{Bat\_max}$: maximum value of battery fractional state of change

$FSOC_{g1\_min}$: minimum fractional state of charge of hydrogen tank of group 1

$FSOC_{g2\_min}$: minimum fractional state of charge of hydrogen tank of group 2

$FSOC_{st}$: fractional state of charge of stationary hydrogen storage tank

i: annual real discount rate

j: replace number of a specific component

J: total replacement number

l_{res}: residual lifetime

l: lifetime of component

n: a certain year

N: service lifetime of hybrid system, year

$P_{Bat\_discharge}$: accessible discharging state of battery

P_{Ele_rated}: rated power of electrolyzer

P_{Load_req}: unmet load to be covered by hydrogen vehicles parking at home

P_i: Pareto optimal solutions

PRV_{costs}: present value of total costs of hybrid system, US$

PRV_{FiT}: present value of feed-in tariff subsidy, US$

PRV_{ini}: present value of initial cost, US$

$PRV_{O\&M}$: present value of operation and maintenance cost, US$

PRV_{rep}: present value of replacement cost, US$

PRV_{res}: present value of residual cost, US$

γ: annual price increasing rate of electricity

δ_{PV}: annual degradation rate of PV system

δ_{WT}: annual degradation rate of wind turbine system

Acknowledgement

The work described in this paper was financially supported by the National Key R&D Program of China: Research and integrated demonstration on suitable technology of net zero energy building (Project No.: 2019YFE0100300). The second author would like to acknowledge the support of the project "1-ZE8B" (The investigation of the multi-objective optimal zero-energy buildings with high energy flexibilities in Hong Kong) in the Hong Kong Polytechnic University for conducting this research.

Reference

[1] Yan J, Yang Y, Campana PE, He J. City-level analysis of subsidy-free solar photovoltaic electricity price, profits and grid parity in China. Nature Energy. 2019;4:709-17.
[2] REN 21. Renewables 2020 global status report. 2020.
[3] Environment Bureau. Hong Kong's Climate Action Plan 2030+. 2017.
[4] Electrical and Mechanical Services Department. Hong Kong Energy End-user Data 2019. 2019.
[5] Liu J, Chen X, Cao S, Yang H. Overview on hybrid solar photovoltaic-electrical energy storage technologies for power supply to buildings. Energy Conversion and Management. 2019;187:103-21.
[6] International Energy Agency. The future of hydrogen: seizing today's opportunities. 2019.
[7] Buttler A, Spliethoff H. Current status of water electrolysis for energy storage, grid balancing and sector coupling via power-to-gas and power-to-liquids: A review. Renewable and Sustainable Energy Reviews. 2018;82:2440-54.
[8] Bruce S, Temminghoff M, Hayward J, Schmidt E, Munnings C, Palfreyman D, et al. National Hydrogen Roadmap. Pathways to an economically sustainable hydrogen industry in Australia. 2018.
[9] Advanced Fuel Cells Technology Collaboration Programme. AFC TCP Survey on the number of fuel cell electric vehicles, hydrogen refuelling stations and targets. 2019.
[10] International Energy Agency. Global EV outlook 2019: overcoming the challenges of transport electrification. 2019.
[11] FuelCells Works. Korean government announces roadmap to become the world leader in the hydrogen economy. 2019.
[12] Strategy Advisory Committee of the Technology Roadmap for Energy Saving and New Energy Vehicles and Society of Automotive Engineers of China. Hydrogen Fuel Cell Vehicle Technology Roadmap. 2016.
[13] California Fuel Cell Partnership. The California fuel cell revolution a vision for advancing economic, social, and environmental priorities. 2018.
[14] Ministry of Economy Trade and Industry Japan. Compilation of the revised version of the strategic roadmap for hydrogen and fuel cells. 2016.
[15] Hydrogen Council. Hydrogen scaling up. A sustainable pathway for the global energy transition. 2017.
[16] Fathabadi H. Novel stand-alone, completely autonomous and renewable energy based charging station for charging plug-in hybrid electric vehicles (PHEVs). Applied Energy. 2020;260:114194.

[17] Robledo CB, Oldenbroek V, Abbruzzese F, van Wijk AJM. Integrating a hydrogen fuel cell electric vehicle with vehicle-to-grid technology, photovoltaic power and a residential building. Applied Energy. 2018;215:615-29.
[18] Cao S, Alanne K. The techno-economic analysis of a hybrid zero-emission building system integrated with a commercial-scale zero-emission hydrogen vehicle. Applied Energy. 2018;211:639-61.
[19] Farahani SS, Bleeker C, van Wijk A, Lukszo Z. Hydrogen-based integrated energy and mobility system for a real-life office environment. Applied Energy. 2020;264:114695.
[20] Clairand J, Arriaga M, Cañizares CA, Álvarez-Bel C. Power Generation Planning of Galapagos' Microgrid Considering Electric Vehicles and Induction Stoves. IEEE Transactions on Sustainable Energy. 2019;10:1916-26.
[21] Cao S. The impact of electric vehicles and mobile boundary expansions on the realization of zero-emission office buildings. Applied Energy. 2019;251:113347.
[22] Huang Z, Xie Z, Zhang C, Chan SH, Milewski J, Xie Y, et al. Modeling and multi-objective optimization of a stand-alone PV-hydrogen-retired EV battery hybrid energy system. Energy Conversion and Management. 2019;181:80-92.
[23] Mohseni S, Brent AC, Burmester D. A comparison of metaheuristics for the optimal capacity planning of an isolated, battery-less, hydrogen-based micro-grid. Applied Energy. 2020;259:114224.
[24] Zhang Y, Campana PE, Lundblad A, Yan J. Comparative study of hydrogen storage and battery storage in grid connected photovoltaic system: Storage sizing and rule-based operation. Applied Energy. 2017;201:397-411.
[25] Mehrjerdi H, Iqbal A, Rakhshani E, Torres JR. Daily-seasonal operation in net-zero energy building powered by hybrid renewable energies and hydrogen storage systems. Energy Conversion and Management. 2019;201:112156.
[26] Mortaz E, Vinel A, Dvorkin Y. An optimization model for siting and sizing of vehicle-to-grid facilities in a microgrid. Applied Energy. 2019;242:1649-60.
[27] Yoon S-G, Kang S-G. Economic microgrid planning algorithm with electric vehicle charging demands. Energies. 2017;10:1487.
[28] Liu J, Chen X, Yang H, Li Y. Energy storage and management system design optimization for a photovoltaic integrated low-energy building. Energy. 2020;190:116424.
[29] The University of Wisconsin Madison. TRNSYS 18. 2017.
[30] Zhou Y, Cao S. Coordinated multi-criteria framework for cycling aging-based battery storage management strategies for positive building–vehicle system with renewable depreciation: Life-cycle based techno-economic feasibility study. Energy Conversion and Management. 2020;226:113473.
[31] Solar Energy Laboratory Univ. of Wisconsin-Madison. TRNSYS 18 a transient system simulation program, Volume 8 weather data. 2017.
[32] Hong Kong Housing Authority. Standard block typical floor plans. 2016.
[33] Hong Kong Electrical and Mechanical Services Department. Guidelines on Performance-based Building Energy Code. 2007.
[34] Wan KSY, Yik FWH. Building design and energy end-use characteristics of high-rise residential buildings in Hong Kong. Applied Energy. 2004;78:19-36.
[35] Chen X, Yang H, Peng J. Energy optimization of high-rise commercial buildings integrated with photovoltaic facades in urban context. Energy. 2019;172:1-17.
[36] Ma T, Yang H, Lu L, Peng J. Optimal design of an autonomous solar–wind-pumped storage power supply system. Applied Energy. 2015;160:728-36.
[37] International Energy Agency Statistics. Electric power transmission and distribution losses (% of output) Hong Kong SAR, China. 2018.
[38] Chen B, Jiang H, Sun H, Yu M, Yang J, Li H, et al. A new gas–liquid dynamics model towards robust state of charge estimation of lithium-ion batteries. Journal of Energy Storage. 2020;29:101343.

[39] Wang D, Cao X. Impacts of the built environment on activity-travel behavior: Are there differences between public and private housing residents in Hong Kong? Transportation Research Part A: Policy and Practice. 2017;103:25-35.
[40] Toyota USA NEWSROOM. Toyota Mirai product information. 2019.
[41] Ramadhani F, Hussain MA, Mokhlis H, Fazly M, Ali JM. Evaluation of solid oxide fuel cell based polygeneration system in residential areas integrating with electric charging and hydrogen fueling stations for vehicles. Applied Energy. 2019;238:1373-88.
[42] Solar Energy Laboratory Univ. of Wisconsin-Madison. TRNSYS 18 a transient system simulation program, Volume 4 mathematical reference. 2017.
[43] Cao S, Alanne K. Technical feasibility of a hybrid on-site H2 and renewable energy system for a zero-energy building with a H2 vehicle. Applied Energy. 2015;158:568-83.
[44] Liu J, Wang M, Peng J, Chen X, Cao S, Yang H. Techno-economic design optimization of hybrid renewable energy applications for high-rise residential buildings. Energy Conversion and Management. 2020;213:112868.
[45] Gökçek M, Kale C. Techno-economical evaluation of a hydrogen refuelling station powered by Wind-PV hybrid power system: A case study for İzmir-Çeşme. International Journal of Hydrogen Energy. 2018;43:10615-25.
[46] Assaf J, Shabani B. Transient simulation modelling and energy performance of a standalone solar-hydrogen combined heat and power system integrated with solar-thermal collectors. Applied Energy. 2016;178:66-77.
[47] Toyota Motor Sales. 2019 Mirai fuel cell electric vehicle. 2020.
[48] Akhtari MR, Baneshi M. Techno-economic assessment and optimization of a hybrid renewable co-supply of electricity, heat and hydrogen system to enhance performance by recovering excess electricity for a large energy consumer. Energy Conversion and Management. 2019;188:131-41.
[49] Jafari M, Armaghan D, Mahmoudi SS, Chitsaz A. Thermoeconomic analysis of a standalone solar hydrogen system with hybrid energy storage. International Journal of Hydrogen Energy. 2019;44:19614-27.
[50] Zhang Y. Use jEPlus as an efficient building design optimisation tool. CIBSE ASHRAE technical symposium2012.
[51] Magnier L, Haghighat F. Multiobjective optimization of building design using TRNSYS simulations, genetic algorithm, and Artificial Neural Network. Building and Environment. 2010;45:739-46.
[52] Lee U, Park S, Lee I. Robust design optimization (RDO) of thermoelectric generator system using non-dominated sorting genetic algorithm II (NSGA-II). Energy. 2020;196:117090.
[53] Chen X, Yang H, Zhang W. Simulation-based approach to optimize passively designed buildings: A case study on a typical architectural form in hot and humid climates. Renewable and Sustainable Energy Reviews. 2018;82:1712-25.
[54] Bingham RD, Agelin-Chaab M, Rosen MA. Whole building optimization of a residential home with PV and battery storage in The Bahamas. Renewable Energy. 2019;132:1088-103.
[55] Electrical and Mechanical Services Department. Introduction to feed-in tariff of renewable energy in Hong Kong. 2018.
[56] Global petrol prices. Hong Kong electricity prices. 2019.
[57] China Light and Power Hong Kong Limited. Electricity price adjustment. 2018.
[58] Campbell M, Aschenbrenner P, Blunden J, Smeloff E, Wright S. The drivers of the levelized cost of electricity for utility-scale photovoltaics. White Paper: SunPower Corporation. 2008.
[59] Li J, Zhang X, Zhou X, Lu L. Reliability assessment of wind turbine bearing based on the degradation-Hidden-Markov model. Renewable Energy. 2019;132:1076-87.
[60] Killer M, Farrokhseresht M, Paterakis NG. Implementation of large-scale Li-ion battery energy storage systems within the EMEA region. Applied Energy. 2020;260:114166.

[61] GlobalData. Further falling inverter prices – market value declining. 2018.
[62] Baldwin D. Development of high pressure hydrogen storage tank for storage and gaseous truck delivery. Hexagon Lincoln LLC, Lincoln, NE (United States); 2017.
[63] Kim I, Kim J, Lee J. Dynamic analysis of well-to-wheel electric and hydrogen vehicles greenhouse gas emissions: Focusing on consumer preferences and power mix changes in South Korea. Applied Energy. 2020;260:114281.
[64] China Light and Power Hong Kong Limited. 2018 Annual report. 2018.
[65] Saaty RW. The analytic hierarchy process—what it is and how it is used. Mathematical modelling. 1987;9:161-76.
[66] Das R, Wang Y, Putrus G, Kotter R, Marzband M, Herteleer B, et al. Multi-objective techno-economic-environmental optimisation of electric vehicle for energy services. Applied Energy. 2020;257:113965.
[67] Chen X, Yang H, Sun K. A holistic passive design approach to optimize indoor environmental quality of a typical residential building in Hong Kong. Energy. 2016;113:267-81.
[68] Freitas Gomes IS, Perez Y, Suomalainen E. Coupling small batteries and PV generation: A review. Renewable and Sustainable Energy Reviews. 2020;126:109835.
[69] International Energy Agency. The Future of Hydrogen. Seizing today's opportunities. 2019.